Records of the Australian Museum (2009) Vol. 61: 1–30. ISSN 0067-1975
doi:10.3853/j.0067-1975.61.2009.1520

Biogeographic and Biostratigraphic Implications of the *Serratognathus bilobatus* Fauna (Conodonta) from the Emanuel Formation (Early Ordovician) of the Canning Basin, Western Australia

YONG YI ZHEN[1]* AND ROBERT S. NICOLL[2]

[1] Australian Museum, 6 College Street, Sydney NSW 2010, Australia
yongyi.zhen@austmus.gov.au

[2] Research School of Earth Science, Australian National University, Canberra ACT 0200, Australia
bnicoll@goldweb.com.au

ABSTRACT. Discovery of *Serratognathus bilobatus* in the Early Ordovician Emanuel Formation of the Canning Basin, Western Australia, has regional biogeographic and biostratigraphic implications. Distribution of *Serratognathus* indicates a close biogeographic link between Australia and adjacent eastern Gondwanan plates and terranes during the latest Tremadocian to early Floian (Early Ordovician), and the formation of the so-called "Australasian Province", a distinctive biogeographic entity that existed throughout most of the Ordovician. The *S. bilobatus* fauna from the Canning Basin is much more diverse in comparison with those assemblages bearing *Serratognathus* from coeval Chinese Lower Ordovician successions and probably represents an assemblage inhabiting relatively deeper water (mid-outer shelf) environments. The Canning Basin fauna contains many pandemic forms, and bridges the gap in the regional correlation of this widely distributed fauna across eastern Gondwana.

This well-preserved, diverse fauna includes *Serratognathus bilobatus* and 23 associated species: *Acodus deltatus?, Acodus? transitans, Bergstroemognathus extensus, Cornuodus* sp., *Drepanodus arcuatus, Drepanoistodus* sp. cf. *D. nowlani, Fahraeusodus adentatus, Lissoepikodus nudus, Nasusgnathus dolonus, Paltodus* sp., *Paracordylodus gracilis, Paroistodus parallelus, Paroistodus proteus, Prioniodus adami, Protopanderodus gradatus, Protoprioniodus simplicissimus, Scolopodus houlianzhaiensis, Semiacontiodus* sp. cf. *S. cornuformis, Stiptognathus borealis, Triangulodus bifidus, Tropodus australis*, gen. et sp. indet. A and gen. et sp. B. A *P. adami-S. bilobatus* Biozone is defined within the middle and upper Emanuel Formation. Correlation of this biozone suggests an early Floian (late *P. proteus* Biozone to possibly earliest *P. elegans* Biozone) age for the middle and upper members of the Emanuel Formation.

ZHEN, YONG YI, & ROBERT S. NICOLL, 2009. Biogeographic and biostratigraphic implications of the *Serratognathus bilobatus* fauna (Conodonta) from the Emanuel Formation (Early Ordovician) of the Canning Basin, Western Australia. *Records of the Australian Museum* 61(1): 1–30.

* author for correspondence

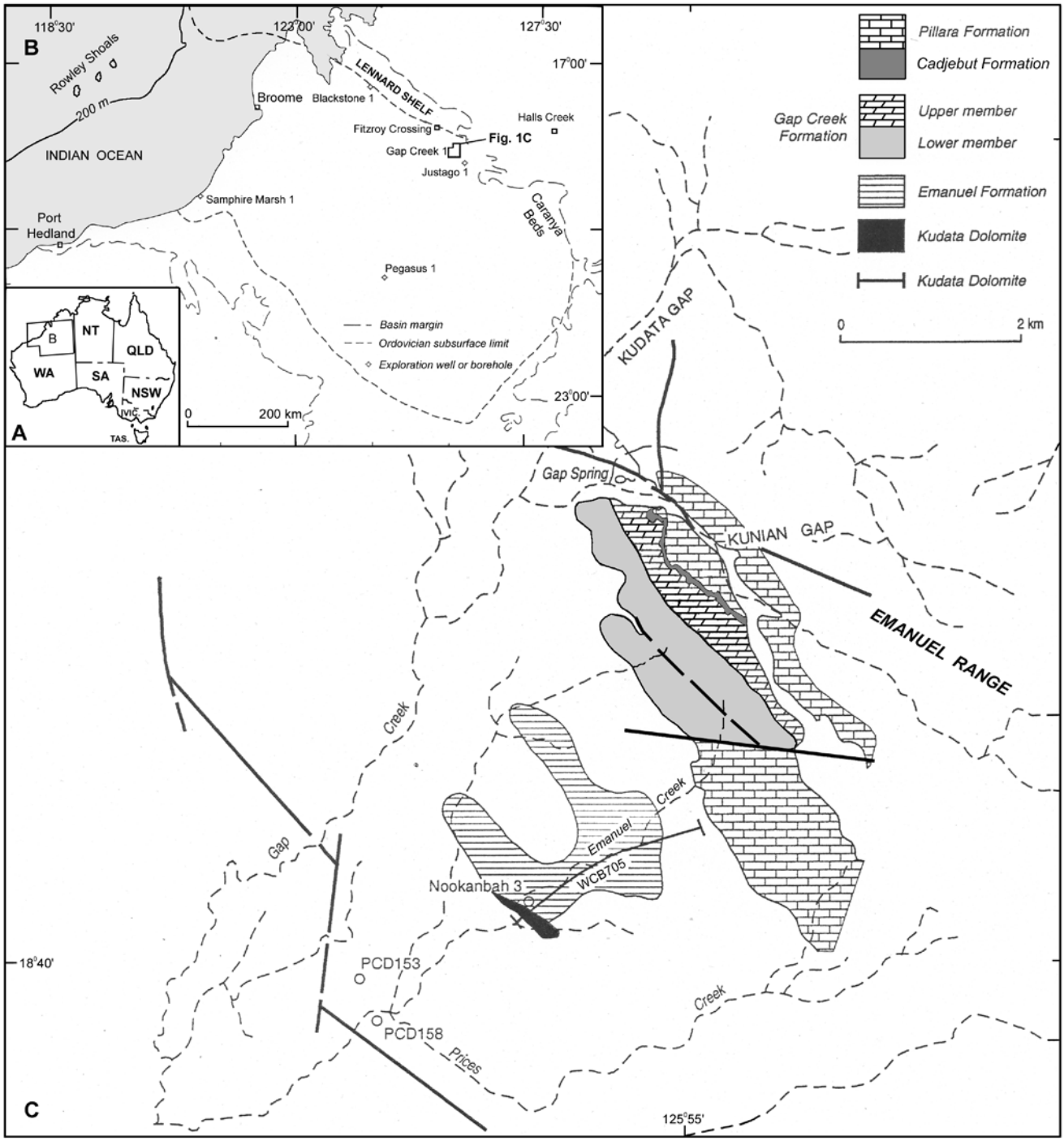

Fig. 1. Localities and geological maps of the studied area. (*A*), map of Australia showing location of the Canning Basin; (*B*), map of the Canning Basin; and (*C*), map of the Emanuel Creek area showing location of section WCB705 along Emanuel Creek (modified from Nicoll *et al*., 1993).

Conodonts are abundant, diverse, and well-preserved in the Early Ordovician Emanuel Formation of the Canning Basin in Western Australia. In the nearly sixty years since the discovery of the fauna (Guppy & Öpik, 1950), this rich fauna has formed the subject of several important studies, particularly on the prioniodontids by McTavish (1973) and by Nicoll & Ethington (2004), rhipidognathids by Zhen *et al*. (2001), *Jumudontus brevis* by Nicoll (1992), and *Stiptognathus borealis* (Repetski, 1982) by Ethington *et al*. (2000). As documentation of the entire fauna represented by a huge collection recovered from several measured sections and subsurface core material is still in progress, the current contribution focuses only on *Serratognathus bilobatus* Lee, 1970 and the associated fauna recovered from three samples of the Emanuel Formation.

The discovery of *S. bilobatus* in the Emanuel Formation, which was deposited in relatively deep water, mid-outer shelf settings, provides crucial new biostratigraphic data to more precisely date and correlate the *Serratognathus* faunas widely distributed in eastern Gondwana and adjacent Peri-

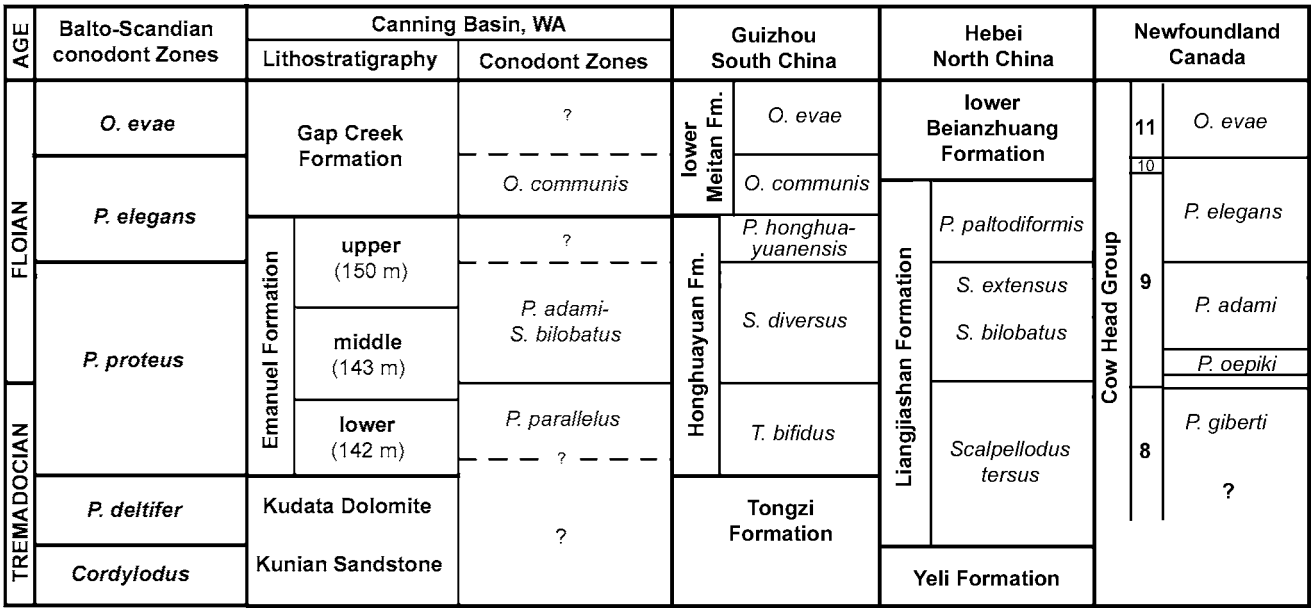

Fig. 2. Conodont biostratigraphy of the Emanuel Formation (late Tremadocian to early Floian, Early Ordovician) of the Canning Basin, and correlation with coeval successions in other regions in South China (Zhen *et al*., in press a), North China (An *et al*., 1983) and western Newfoundland (Stouge & Bagnoli, 1988).

Gondwanan plates and terranes. Regional correlation with coeval *Serratognathus*-bearing faunas from the Arafura Basin and from China, Korea and Malaysia, defines a distinctive Australasian Province in eastern Gondwana (Zhen *et al*. in Webby *et al*., 2000) during the latest Tremadocian to early Floian (Early Ordovician). Moreover, as the *S. bilobatus* fauna from the Emanuel Formation contains a number of pandemic species, it serves as an ideal bridge correlating the *S. bilobatus* faunas in China and the more intensively studied Balto-Scandian and North American Mid-continent successions.

Regional geological setting and lithostratigraphy

The Canning Basin is an intracratonic sag basin, bounded by Precambrian rocks of the Kimberley Block to the north and the Pilbara Block to the south, occupying about one-sixth of Western Australia's onshore area (Fig. 1). Sparsely inhabited and covered largely by flat-topped hills and sand dunes, it is dominated by a Palaeozoic-Mesozoic sedimentary succession more than 15 km in thickness. Extensive geological investigations have been carried out in the region for more than a century (Purcell, 1984), spurred on by its high potential for fossil fuel reserves.

The Early Ordovician Prices Creek Group, representing the oldest stratigraphic unit in the basin, is only exposed along its northern margin (Lennard Shelf) where it rests unconformably on Precambrian basement. This basal contact is observable only in drillcore. The Prices Creek Group is overlain paraconformably by the Middle Devonian (Givetian) Cadjebut Formation (Hocking *et al*., 1996). The group was initially subdivided into a lower Emanuel Limestone (subsequently renamed Emanuel Formation) and an upper Gap Creek Dolomite (later amended to Gap Creek Formation) with a measured thickness of 595 m for the Emanuel Formation in the type section along Emanuel Creek (Guppy & Öpik, 1950; Guppy *et al*., 1958). Exploration drill holes in the area revealed an additional unexposed section between the Emanuel Formation and metamorphic rocks of the Precambrian basement, comprising a dolomitic interval 88 m thick underlain by 82 m of arkose (Veevers & Wells, 1961; Henderson, 1963; McTavish & Leg, 1976; Towner & Gibson, 1983). Nicoll *et al*. (1993) formally named the dolomitic unit the Kudata Dolomite and the arkose unit the Kunian Sandstone, and revised the Emanuel Formation as consisting of limestone intercalated with shale and siltstone with a total thickness of 435 m exposed in the type section (Fig. 1).

Regionally the Emanuel Formation conformably overlies the Kudata Dolomite and is conformably overlain by the Gap Creek Formation of mid-late Floian age (Fig. 2). The basal arkose of the Kunian Sandstone was deposited in a major transgressive phase flooding the Canning Basin during the Tremadocian (Nicoll *et al*., 1993). This age determination was based on the regional tectonic framework and event stratigraphy, as well as fossil evidence from the overlying Kudata Dolomite, as no fossils were found in the arkose unit. The Emanuel Formation was subdivided into three informal members (Nicoll *et al*., 1993). However, in the type area, both lower and upper members with intercalated shale, siltstone and limestone (or nodular limestone in the upper member) are poorly exposed, whereas the limestone-dominated middle member with a thickness of 143 m is better exposed forming a more or less continuous section. The Emanuel Formation has not only yielded a rich conodont fauna, but also trilobites (Legg, 1976; Laurie & Shergold, 1996a, 1996b), graptolites (Thomas, 1960; Legg, 1976), nautiloids (Teichert & Glenister, 1954), gastropods (Gilbert-Tomlinson, 1973; Jell *et al*., 1984; Yu, 1993), brachiopods (Brock & Holmer, 2004) and various other invertebrate and microfossil groups (Guppy & Öpik, 1950; Brown, 1964; Schallreuter, 1993a, 1993b).

Table 1. Distribution of conodont species recovered from three samples in the Emanuel Formation of the Canning Basin, Western Australia.

species	WCB705/133	WCB705/243	161–166 m	Total
Acodus deltatus?	14	185	10	209
Acodus? transitans	4			4
Bergstroemognathus extensus	32	71		103
Cornuodus sp.	7	12	4	23
Drepanodus arcuatus	65	19	11	95
Drepanoistodus sp. cf. *D. nowlani*	30	13	9	52
gen. et sp. indet. A	10			10
gen. et sp. indet. B	1			1
Fahraeusodus adentatus	1		6	7
Lissoepikodus nudus	28	19	2	49
Nasusgnathus dolonus	19	6	5	30
Paracordylodus gracilis		35		35
Paltodus sp.	1			1
Paroistodus parallelus	180	256	21	457
Paroistodus proteus	16	12	2	30
Prioniodus adami	1	3		4
Protopanderodus gradatus	2	124		126
Protoprioniodus simplicissimus	8	17	3	28
Scolopodus houlianzhaiensis	3	5	11	19
Semiacontiodus sp. cf. *S. cornuformis*	18	4	4	26
Serratognathus bilobatus	5	1	1	7
Stiptognathus borealis	4	103		107
Triangulodus bifidus	1	2		3
Tropodus australis	77	83	30	190
total	527	970	119	1616

Age and correlation of the conodont fauna

McTavish (1973) described 20 multi-element conodont species and subspecies from the Emanuel Formation and lower part of the Gap Greek Formation; 19 of these were referred to prioniodontid genera, namely *Acodus, Baltoniodus, Prioniodus* and *Protoprioniodus*, and one to Periodontidae. On the basis of correlation with Balto-Scandian and North America Mid-continent successions McTavish (1973) determined a Latorpian age (latest Tremadocian to Floian in current terminology) for the Emanuel Formation and lower Gap Creek Formation. In particular, occurrence of *Acodus deltatus*?, *Paroistodus proteus* and *P. parallelus* in the Emanuel Formation allowed its correlation with the *Paroistodus proteus* Biozone (Hunneberg) of the Balto-Scandian succession, and the appearance of *Oepikodus communis* in the lower Gap Creek Formation supported correlation with the Ninemile Formation of central Nevada (McTavish, 1973, pp. 31, 32), namely the *O. communis* Biozone of the North America Mid-continent succession.

In our study 24 conodont species are documented from three samples in the middle and upper members of the Emanuel Formation (Table 1). *Paroistodus parallelus*, *Acodus deltatus*?, *Tropodus australis, Protopanderodus gradatus, Stiptognathus borealis, Bergstroemognathus extensus*, and *Drepanodus arcuatus* dominate the fauna, whereas *Serratognathus bilobatus* is relatively rare. As shown in Table 2, among the 24 species recorded in this study, 11 species were also recorded in the Honghuayuan Formation in the Yangtze Platform of South China (An, 1987, Ding *et al*. in Wang, 1993; Zhen *et al*., in press a), seven in the Liangjiashan Formation of the North China Platform (An *et al*., 1983), only three in the Qianzhongliangzi Formation of the Ordos Basin of North China Plate (An & Zheng, 1990), and four in the upper subgroup of the Qiulitag Group of the Tarim Basin (Zhao *et al*., 2000). Recently a fauna closely comparable with that documented herein (with 12 species in common including *S. bilobatus*) was found in the Mooroongga Formation in the offshore Arafura Basin, north Australia (Nicoll unpublished material), indicating wide distribution of this species in western and northern Australia.

Jumudontus brevis Nicoll, 1992 ranges from the middle member to lower part of the upper member of the Emanuel Formation. It is a pandemic species, also found in Early Ordovician rocks in Utah and Texas (Ethington & Clark, 1982), Newfoundland (Stouge & Bagnoli, 1988), western Canada (Norford *et al*., 2002), Baltoscandia (Bergström, 1988) and Greenland (Smith, 1991). In the Fillmore Formation of Utah, *J. brevis* first appears three m above the FAD of *O. communis* and extends to 237.7 m above the base of the formation at section H, suggesting a correlation with the lower *O. communis* Biozone (Ethington & Clark, 1982). In Newfoundland, it occurs in the upper part of Bed 9 (upper *P. elegans* Biozone) and lower part of Bed 11 (*O. evae* Biozone) of the Cow Head Group (Stouge & Bagnoli, 1988), an interval slightly higher than its occurrence (= upper *P. proteus* Biozone to lower *P. elegans* Biozone) in the Emanuel Formation.

Stiptognathus borealis (Repetski, 1982) is present from the upper part of the middle member to the basal part of the upper member of the Emanuel Formation, a range slightly shorter than that of *J. brevis* (Ethington *et al*., 2000; Nicoll & Ethington, 2004). It was also recorded from the Great Basin (Ethington & Clark, 1982; Ethington *et al*., 2000), western

Table 2. Comparison of occurrence of conodont species of the *Serratognathus* fauna from the Emanuel Formation with their distribution in other *Serratognathus* faunas recognized in China and other coeval successions referred to in the text.

species	mid-upper part of Emanuel Formation	Mooroongga Formation Arafura Basin	*S. diversus* Zone South China	*S. bilobatus* Zone North China	mid Qian-zhongliangzi Formation Ordos Basin	Qiulitag Group Tarim Basin	upper Dakui Formation Hainan	Setul Limestone Malaysia	*P. adami* Zone Bed 9 Newfoundland
Acodus deltatus?	•	•							
Acodus? transitans	•								
Bergstroemognathus extensus	•	•	•	•	•	•			•
Cornuodus sp.	•								
Drepanodus arcuatus	•	•	•	•					•
Drepanoistodus sp. cf. *D. nowlani*	•		•						
gen. et sp. indet. A	•								
gen. et sp. indet. B	•								
Fahraeusodus adentatus	•								
Lissoepikodus nudus	•	•							
Nasusgnathus dolonus	•	•	•	•		•			
Paracordylodus gracilis	•								•
Paltodus sp.	•								
Paroistodus parallelus	•						•		•
Paroistodus proteus	•	•	•	•					•
Prioniodus adami	•	•?							•
Protopanderodus gradatus	•	•	•	•					•
Protoprioniodus simplicissimus	•	•	•						•
Scolopodus houlianzhaiensis	•	•	•	•	•		•		
Semiacontiodus sp. cf. *S. cornuformis*	•		•						
Serratognathus bilobatus	•	•	•	•	•	•	•	•	
Stiptognathus borealis	•								
Triangulodus bifidus	•	•	•			•			
Tropodus australis	•								•

Texas (Repetski, 1982), and the Argentine Precordillera (Lehnert, 1995; Albanesi in Albanesi *et al*., 1998). According to Ethington *et al*. (2000), it occurs in the Fillmore Formation of Utah, in the upper quarter of the El Paso Group and in the upper member of the Marathon Limestone of Texas, and in the Mountain Springs Formation of Nevada, constrained within an interval of upper *Acodus deltatus/Oneotodus costatus* Biozone to lower *O. communis* Biozone (early Floian age). However, in the Argentine Precordillera, earliest occurrence of *S. borealis* occurs in the upper *P. proteus* Biozone within the Tremadocian/Floian boundary interval.

Scolopodus houlianzhaiensis An & Xu in An *et al*., 1983 occurs abundantly in the Liangjiashan Formation of North China with a similar stratigraphic range to that of *Serratognathus bilobatus* (An *et al*., 1983), and was also reported from the Honghuayuan Formation in Guizhou (South China) in association with *Serratognathus diversus* (Zhen *et al*., in press a). As both the Liangjiashan Formation and Honghuayuan Formation were deposited in shallow subtidal settings, faunas recovered from these two units are dominated by endemic forms, and it is difficult to directly correlate them with either the Balto-Scandian or North American Mid-continent successions. Thus the presence of *S. houlianzhaiensis* in association with *Serratognathus bilobatus* in the Emanuel Formation is critical to bridging this correlation gap.

Triangulodus bifidus Zhen in Zhen *et al*., 2006 is a morphologically distinctive species occurring throughout the Honghuayuan Formation and also into the lower part of the overlying Meitan Formation in South China (Zhen *et al*., 2006, 2007a). It is apparently a rare species in the Emanuel Formation, represented by only a few specimens (Fig. 15I–K), and will be reported from the *S. bilobatus* fauna in the Arafura Basin of northern Australia (Nicoll unpublished material).

Co-occurrence of *Paroistodus proteus* and *P. parallelus* in the Emanuel Formation also suggests a correlation with the upper part of the *P. proteus* Biozone of the Balto-Scandian succession. Löfgren (1997) indicated that in Sweden, *Paroistodus parallelus* makes its first appearance in the uppermost *P. proteus* Biozone, often associated with *P. proteus*, and extends to the upper middle *O. evae* Biozone. More specifically, occurrence of *Prioniodus adami* in the upper part of the Emanuel Formation allows a direct correlation with the *P. adami* Biozone (= upper *P. proteus* Biozone) recognized in the Cow Head Group of Newfoundland (Stouge & Bagnoli, 1988). There, *P. adami* was reported ranging through the lower to upper part (but not top) of Bed 9 in the Ledge-Point of Head Section (Stouge & Bagnoli, 1988, fig. 3), and the *P. adami* Biozone (succeeded by the *P.*

elegans Biozone) is characterized by abundant *P. adami* in association with *Bergstroemognathus extensus*, *Drepanodus arcuatus*, *Paroistodus parallelus*, *P. proteus*, *Paracordylodus gracilis*, *Tropodus australis*, *Protopanderodus gradatus*, and *Protoprioniodus simplicissimus*, all of which are also present in the Emanuel Formation. According to Stouge & Bagnoli (1988, figs 3,4), both *O. communis* and *P. elegans* first appear at a similar level in the upper part (not top) of Bed 9 and define the boundary of the *P. adami*/*P. elegans* biozones in the upper part of Bed 9. Both *P. proteus* and *P. parallelus* make their first appearance near the base of Bed 9 of the Cow Head Group, about three m below the first appearance of *P. adami*.

The first appearance (FAD) of *Tetragraptus approximatus* is the primary marker defining the base of the Floian Stage (Bergström *et al*., 2004). In the Diabasbrottet GSSP Section at Hunneberg, southwestern Sweden, the Tremadocian/Floian boundary was defined by the FAD of *T. approximatus*, 2.1 m above the top of the Cambrian, and the lower part of the *T. approximatus* graptolite Biozone was correlated to the topmost subzone (*Oelandodus alongatus-Acodus deltatus deltatus* Subzone) of the *P. proteus* conodont Biozone (see Bergström *et al*., 2004, fig. 10). Therefore, the FAD of *T. approximatus* near the base (3m above the base at the Ledge Section) of Bed 9 in the Cow Head Group (Williams *et al*., 1999) suggests that the *P. adami* Biozone in Newfoundland should be correlated with the upper part of the *P. proteus* Biozone (*Oelandodus alongatus-Acodus deltatus deltatus* Subzone) of the Balto-Scandian succession.

The *P. adami-S. bilobatus* Biozone is proposed herein to represent the fauna from the middle to upper part of the Emanuel Formation. It is characterized by the occurrence of *P. adami*, *S. bilobatus, Paroistodus proteus, P. parallelus* and other species listed in Table 1, with its base defined by the first appearance of *S. bilobatus* from the middle member of the Emanuel Formation and the upper boundary defined by the first appearance of *O. communis* in the basal part of the Gap Creek Formation (Nicoll & Ethington, 2004). It can be confidently correlated with the *P. adami* Biozone in the lower part of Bed 9 of the Cow Head Group in Newfoundland, with the *Oelandodus alongatus-Acodus deltatus deltatus* Subzone of the *P. proteus* Biozone (possibly also lowest *P. elegans* Biozone) of the Balto-Scandian conodont succession, with the *S. diversus* Biozone in the Honghuayuan Formation of South China, and with the *S. bilobatus* and *S. extensus* biozones in the Liangjiashan Formation of North China (Fig. 2).

Biogeographic distribution of *Serratognathus*

The morphologically distinctive conodont *Serratognathus* is widely distributed in Lower Ordovician (lower Floian) rocks in China (South China, North China Platform, Ordos Basin, Tarim Basin and southern Hainan Island), Korea, Malaysia, and Australia (Arafura Basin and Canning Basin). Among the three species assigned to the genus (*S. bilobatus* Lee, 1970, *S. diversus* An, 1981, and *S. extensus* Yang in An *et al*., 1983), *S. bilobatus* has a relatively wider geographic distribution (Fig. 3) occurring in the Dumugol Formation of South Korea (Lee, 1970), in the Liangjiashan Formation of North China Platform (An *et al*., 1983), in the Qianzhongliangzi Formation of the Ordos Basin in North China (An & Zheng, 1990), in the Honghuayuan Formation of South China (An *et al*., 1983; Ding *et al*. in Wang, 1993), in the upper part of the Dakui Formation of Sanya, Hainan Island (Wang *et al*., 1996), in the lower part of the Setul Limestone in Malaysia (Metcalfe, 1980, 2004), in the Mooroongga Formation (subsurface) of the Arafura Basin off the north coast of Australia (Nicoll unpublished material), and in the Emanuel Formation of the Canning Basin, Western Australia (this study). Zhylkaidarov (1998, p. 65) indicated the occurrence of *S. bilobatus* from the Shabakty Formation in Malyi Karatau of southern Kazakhstan. However, as neither illustrations nor other information of the species from this locality are available, this Kazakhstan occurrence is considered doubtful at present. *Serratognathus diversus* is recorded in the Honghuayuan Formation and coeval units in South China (An *et al*., 1985; An, 1987; Zhen *et al*., in press a), Liangjiashan Formation of North China (An *et al*., 1983), and the upper subgroup of the Qiulitag Group of the Tarim Basin (Zhao *et al*., 2000). *Serratognathus extensus*, possibly representing the most advanced of the three species, has been reported only from the Liangjiashan Formation of North China Platform (An *et al*., 1983).

The type material of *S. bilobatus* was described from the Dumugol Formation in the Taebaeksan Basin in the central-eastern part of the Korean Peninsula (Lee, 1970; Choi *et al*., 2005). The Dumugol Formation (also called the Dumugol Shale) consists of shale and intercalated limestone whose thickness varies from 150 to 270 m across the region and contains cyclic successions shifting from the near-shore to the deeper subtidal facies on a low-relief carbonate shelf, which was believed to be part of an extension of the North China Platform during the Early Ordovician (Choi *et al*., 2001, 2005). It yielded abundant conodont and trilobite faunas closely comparable to the late Tremadocian to early Floian faunas of North China (Lee, 1970, 1975; An *et al*., 1983; Zhou & Fortey, 1986; Seo *et al*., 1994; Choi *et al*., 2005). Occurrence of the *Archaeoscyphia-Calathium* association (occasionally forming isolated bioherms) in the Dumugol Formation also supports a close biogeographic link with North China (Choi *et al*., 2005). Based on rich and diverse conodont assemblages, Seo *et al*. (1994) divided the Dumugol Formation into four conodont biozones (in ascending order): *Chosonodina herfurthi-Rossodus manitouensis* Biozone, *Colaptoconus quadraplicatus* Biozone, *Paracordylodus gracilis* Biozone, and *Triangulodus dumugolensis* Biozone, with an age ranging from late Tremadocian to early Floian. They correlated the *Triangulodus dumugolensis* Biozone at the top of the Formation to the *S. bilobatus* Biozone of North China, but unfortunately *S. bilobatus* was not recovered from any of their studied samples, and the type horizon of this species described by Lee (1970) in the region was not pinned down in their new biostratigraphic scheme of the Dumugol Formation. However, Seo *et al*. (1994, p. 606) indicated that *S. bilobatus* also occurs in the overlying Maggol Formation as reported in two unpublished postgraduate theses.

In North China, *S. bilobatus* was widely reported as occurring in the Liangjiashan Formation within an interval correlated to the upper *P. proteus* Biozone to lower *P. elegans* Biozone of the Balto-Scandian conodont succession (Zhen *et al*., in press a). The Liangjiashan Formation is best exposed in the Zhaogezhuang Section near Tangshan, Hebei Province, where it consists of a 160 m sequence of a thick-bedded lower limestone member and an upper dolomite member (Chen Xu *et al*., 1995) that conformably overlies the Yeli (Yehli) Formation of Tremadocian age and is overlain by the Beianzhuang Formation of the

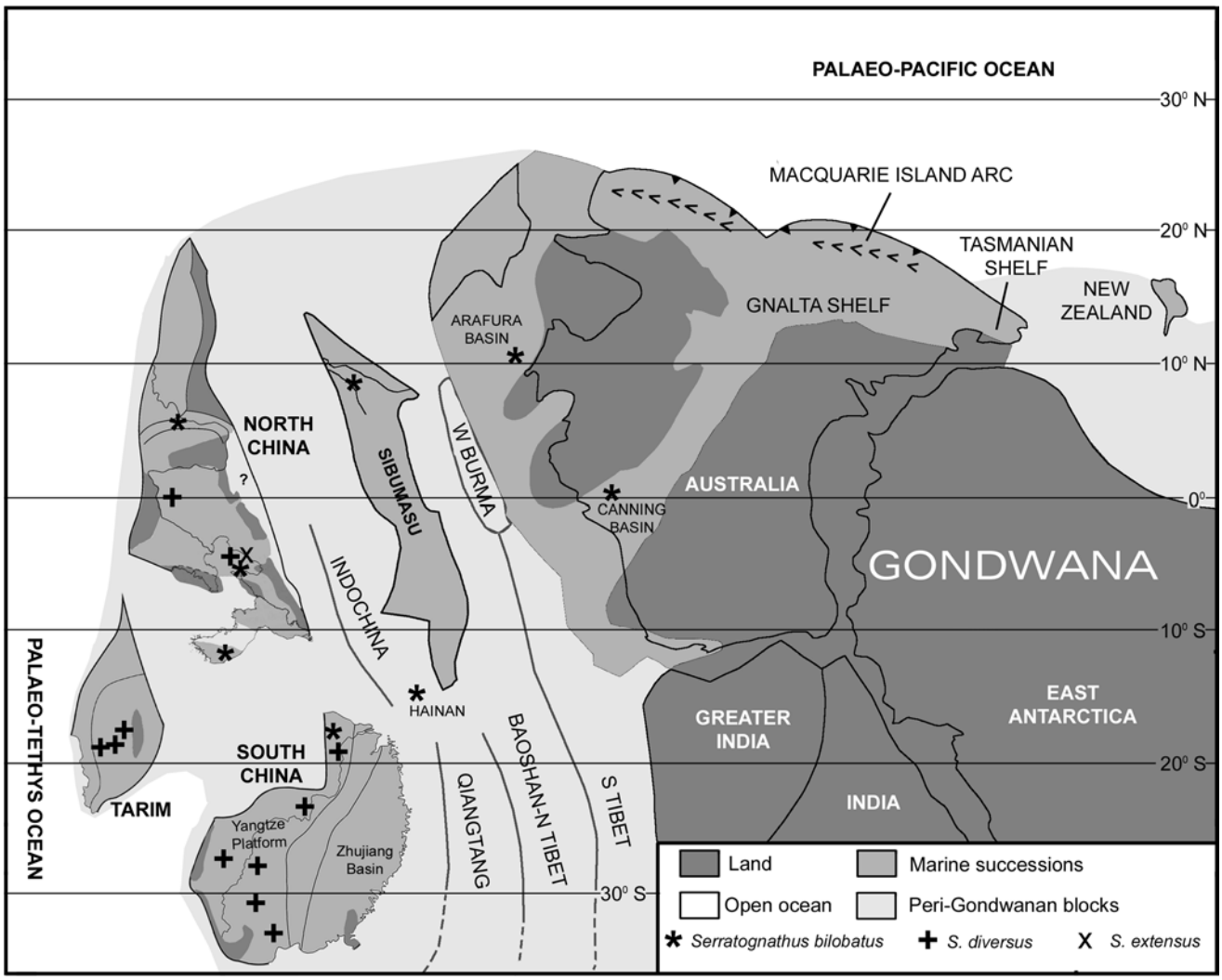

Fig. 3. Early Floian palaeobiogeographic reconstruction of eastern Gondwana (after Nicoll *et al*., 1993; Webby *et al*., 2000; Huang *et al*., 2000).

late Floian to Dapingian age. An *et al*. (1983) subdivided the formation into four conodont biozones (in ascending order): (*1*) *Scalpellodus tarsus* Biozone; (*2*) *Serratognathus bilobatus* Biozone; (*3*) *Serratognathus extensus* Biozone; and (*4*) *Paraserratognathus paltodiformis* Biozone. The *S. bilobatus* Biozone is confined to the lower part of the Liangjiashan Formation with a total thickness of 30 m in the Zhaogezhuang Section; the overlying *S. extensus* Biozone ranges through the middle part of the formation with a total thickness of 50 m (An *et al*., 1983, p. 26).

In the Honghuayuan Formation (the coeval strata on the Yangtze Platform of South China), *S. bilobatus* is rare and has been reported only from the Lower Yangtze Valley (An & Ding, 1982, 1985). A closely related species, *S. diversus*, is dominant in the fauna. Recent studies (Zhen *et al*., in press *a*) of the conodonts from the Honghuayuan Formation at its type locality and several other sections in Guizhou resulted in the recognition of three conodont biozones in the Formation (in ascending order): *Triangulodus bifidus* Biozone, *Serratognathus diversus* Biozone and *Prioniodus honghuayuanensis* Biozone. In the type section of the Honghuayuan Formation, *S. diversus* is confined to an interval of 13.5 m in the middle part of the Formation which is correlated to the upper *P. proteus* Biozone of the Balto-Scandian succession (Zhen, 2007, Zhen *et al*. in press *a*).

When correlating the conodont fauna from the Emanuel Formation and the lower Gap Creek Formation with well-studied Balto-Scandian and North America Mid-continent conodont successions, McTavish (1973, p. 31) was puzzled by the fact that Balto-Scandian Lower Ordovician successions were condensed, while North America Mid-continent successions, although with "comparable thickness to the Emanuel Formation" had faunas "of limited value for precise age determination". At the time, he did not attribute these faunal differences and difficulties in correlation to either ecological or biogeographical reasons. It is now understood that distribution of conodont animals was largely controlled by the water temperature and the water depth of their habitats (see Zhen & Percival, 2003). Higher resolution of the faunal correlation can only be achieved by comparing faunas from the same biogeographical province and Domain or at least from the same realm, otherwise ecological and biogeographical overprints should be removed or discounted when comparing faunas from different biogeographical settings.

A restricted distribution of *Serratognathus* in eastern Gondwana (Fig. 3) strongly supports the concept that the so-called "Australasian Province" became evident in the latest Tremadocian and early Floian, and persisted through

most of the Ordovician (Nowlan *et al*., 1997; Zhen *et al*. in Webby *et al*., 2000). Restriction of *S. diversus* primarily to the South China and the Tarim plates also indicates a closer biogeographic relationship between these two Chinese plates in the early Floian, and agrees with the recent biogeographic analysis based on the trilobite geographical and stratigraphical distribution data from the Chinese Cambrian (Zhou *et al*., 2008) and Ordovician (Zhou & Zhen, 2008). Trilobite data (Zhou & Zhen, 2008; Zhou *et al*., 2008) suggested that a broad undifferentiated biogeographic entity persisted in the Chinese plates and terranes positioned in eastern Gondwana from Cambrian to Tremadocian time, and became more diversified in the early Floian when two subprovinces (North China and South China) could be recognized (Zhou *et al*., 2008, fig. 2). Trilobite distributional patterns and sharing of several endemic forms also support a closer biogeographic tie between Australia and North China (Choi *et al*., 2001; Zhou & Zhen, 2008; Zhou *et al*., 2008).

Material and methods

All photographic illustrations shown in Figs 4 to 16 are SEM photomicrographs captured digitally (numbers with the prefix IY are the file names of the digital images). Conodont specimens for this study are from three samples from the Emanuel Formation that bear *S. bilobatus*. Both WCB705/133 and WCB705/243 are from Section WCB 705 measured by following the line of the type section (Guppy & Öpik, 1950; Grid Ref. for base: 18°39'50"S 125°54'00"E; and top: 18°39'12"S 125°55'05"E), and sample 161–166 m is from a drillhole (BHP/PDH, grid ref. 18°40'30"S 125°33'00"E, from the middle part of the Emanuel Formation, see Nicoll *et al*., 1993) in the northern margin of the Canning Basin. Figured specimens bearing the prefix CPC are housed in the Palaeontology Collection of Geoscience Australia in Canberra. Those bearing the prefix "AM F" (Figs 12–14) are deposited in the collections of the Palaeontology Section at the Australian Museum, Sydney, and were collected from the Honghuayuan Formation in Guizhou (see Zhen *et al*. in press a for sampling locations and stratigraphic details). Several species documented herein only by illustration are rare in the collection [*Cornuodus* sp. (Fig. 4G–L), gen. et sp. indet. A (Figs 8L–O, 10Y), *Nasusgnathus dolonus* (An, 1981) (Fig. 10S–U), *Paltodus* sp. (Fig. 10X), *Protoprioniodus simplicissimus* McTavish, 1973 (Fig. 6M–R), gen.sp. indet. B (Fig. 10W), and *Triangulodus bifidus* Zhen in Zhen *et al*., 2006 (Fig. 15I–K)] or those which are discussed adequately elsewhere [*Bergstroemognathus extensus* (Graves & Ellison, 1941) (see Zhen *et al*., 2001; Fig. 4A–F), *Lissoepikodus nudus* Nicoll & Ethington, 2004 (see Nicoll & Ethington, 2004; Fig. 10L–R), and *Stiptognathus borealis* (Repetski, 1982) (see Ethington *et al*., 2000; Fig. 15A–H)]. Conodont terminology and notation employed in this contribution are conventional as defined in Treatise Part W (Clark *et al*., 1981), except for the M elements (makellate), whose orientation, morphology and the terminology was introduced by Nicoll (1990, 1992).

Systematic palaeontology

Phylum Chordata Balfour, 1880

Class Conodonta Pander, 1856

Acodus Pander, 1856

Diaphorodus Kennedy, 1980: 51.

Type species. *Acodus erectus* Pander, 1856.

Remarks. The name *Acodus*, although widely cited in Ordovician conodont literature, has been a subject of debate and has remained one of the most controversial conodont genera for many years. As its type species *A. erectus* was poorly known, Kennedy (1980) regarded *Acodus* as a *nomen dubium*, and this view was accepted by several subsequent workers (e.g., Sweet, 1988), while others (e.g., Lindström in Ziegler, 1977; Ji & Barnes, 1994; Zhen *et al*., 2004) retained *Acodus* as a valid genus, but with varying definitions.

During the late Tremadocian to early Floian, conodonts evolved rapidly and experienced the greatest diversification event in their evolutionary history of some 300 million years. Several important clades, particularly the Prioniodontida, evolved from forms previously gouped with *Acodus*. Understanding of the apparatus composition and structure of *Acodus* and related taxa is crucial in depicting the phylogenetic relationships and evolutionary history of these related clades (Stouge & Bagnoli, 1999). Therefore, a narrower rather than broader generic concept is needed for *Acodus*, which is restricted herein to forms with the same apparatus composition and structure as *Prioniodus* but typically consisting of adenticulate elements.

Recent study by Nicoll & Ethington (2004) shows that Oepikodontidae diverged from the main clade of Prioniodontoidea in the late Tremadocian through an adenticulate stage represented by *Lissoepikodus* (recognized in the Emanuel Formation), and supports the hypothesis that both Prioniodontoidea and Balognathoidea might have evolved from a common ancestor (Stouge & Bagnoli, 1999), most likely *Acodus* (= *Diaphorodus* + "*Acodus*" *deltatus* of Stouge & Bagnoli, 1999).

As Pander's type specimens of the genotype, *A. erectus*, are lost, our current understanding of *Acodus* is largely based on several subsequent works on *A. deltatus* Lindström, 1955 and other related species documented by McTavish (1973),

[Fig. 4, caption continued]. (*G*), P element (short based), CPC39796, inner lateral view (IY129-024). *H–J*, Sa element; (*H*), CPC39797, lateral view (IY129-009); (*I*), CPC39798, lateral view (IY129-11); (*J*), CPC39799, basal view (IY129-014). (*K*), P element (short based), CPC39800, inner lateral view (IY129-020). (*L*), Sb element, CPC39801, inner lateral view (IY129-018). *M–R*, *Acodus*? *transitans* McTavish, 1973. *M–Q*, Pa element; M,N, CPC39802; (*M*), basal-outer lateral view (IY126-018); (*N*), outer lateral view (IY126-020). (*O*), CPC39803, inner lateral view (IY126-029). *P–R*, Sc element; P,Q, CPC39804; (*P*), outer lateral view (IY126-021); (*Q*), basal-outer lateral view (IY126-022); (*R*), CPC39805, outer lateral view (IY126-023). *S–X*, *Acodus deltatus*? Lindström, 1955. (*S*), M element, CPC39806, 161–166 m, posterior view (IY130-034); (*T*), Sb element, CPC39807, WCB705/243, outer lateral view (IY130-045); (*U*), Sd element, CPC39808, 161–166 m, inner lateral view (IY132-010); *V–X*, P element; V,W, CPC39809, 161–166 m; (*V*), anterior view (IY130-037); (*W*), inner lateral view (IY130-038); (*X*), CPC39810, 161–166 m, outer lateral view (IY130-028). Scale bars 100 μm.

Fig. 4. A–F, *Bergstroemognathus extensus* (Graves & Ellison, 1941). All from sample WCB705/243. (*A*), M element, CPC39790, posterior view (IY116-046). (*B*), Sa element, CPC39791, posterior view (IY116-047). (*C*), Sb element, CPC39792, inner lateral view (IY116-048). (*D*), Sc element, CPC39793, inner lateral view (IY116-049). (*E*), Pb element, CPC39794, inner lateral view (IY116-042). (*F*), Pa element, CPC39795, inner lateral view (IY116-043). *G–L*, *Cornuodus* sp. All from WCB705/243; …[continued on facing page]

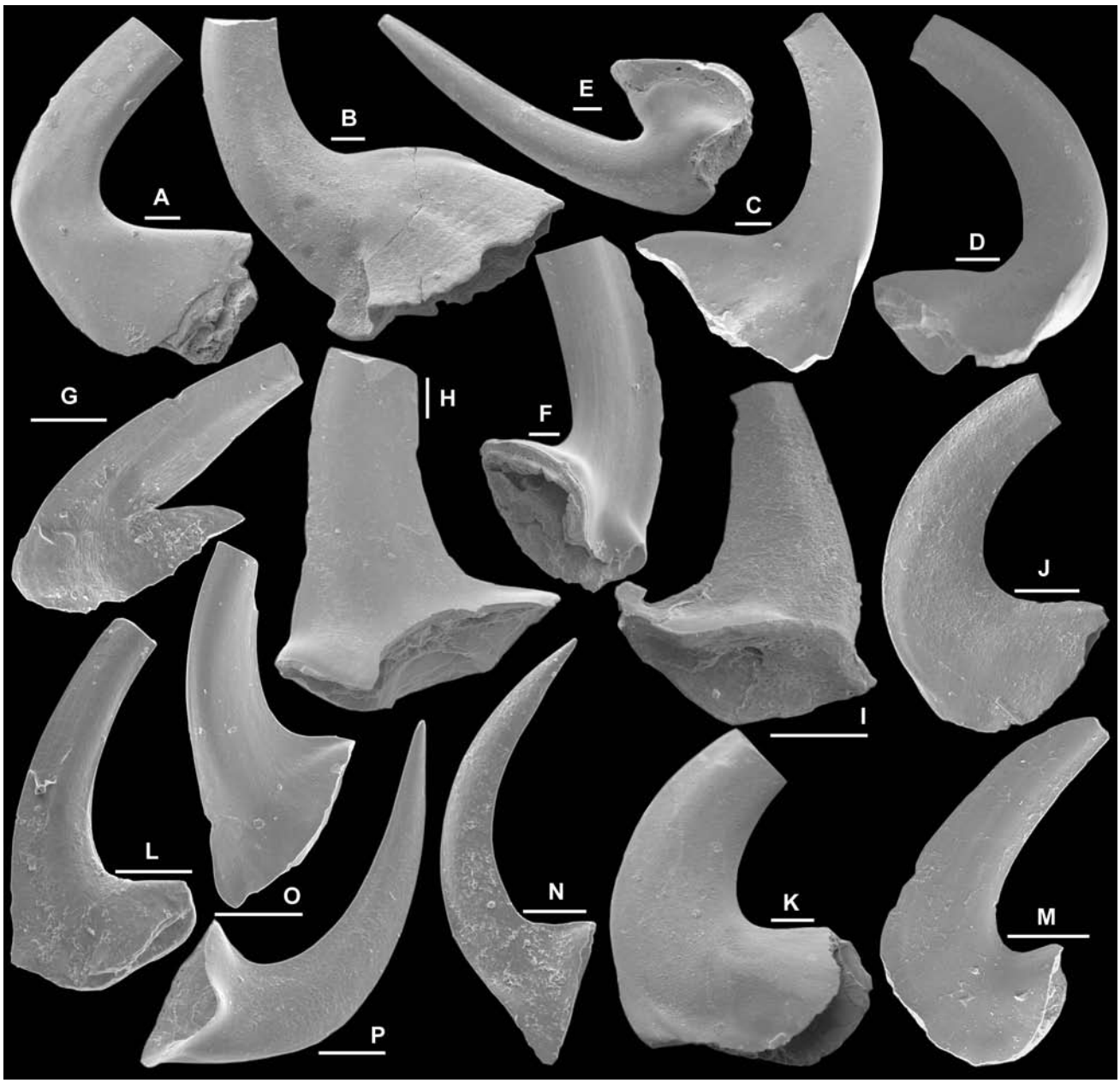

Fig. 5. *A–F*, *Drepanodus arcuatus* Pander, 1856. All from sample WCB705/133. A,B, Sa element; (*A*), CPC39811, lateral view (IY126-002); (*B*), CPC39812, lateral view (IY126-003). *C,D*, Sd element; (*C*), CPC39813, inner lateral view (IY127-028); (*D*), CPC39814, inner lateral view (IY127-022). (*E*), Pb element, CPC39815, inner lateral view (IY126-001). (*F*), Pa element, CPC39816, outer lateral view (IY126-005). *G–P*, *Drepanoistodus* sp. cf. *D. nowlani* Ji & Barnes, 1994. (*G*), M element, CPC39817, WCB705/243, anterior view (IY129-005). *H,I*, Sa element; (*H*), CPC39818, WCB705/133, lateral view (IY126-004); (*I*), CPC39819, WCB705/133, lateral view (IY127-016). (*J*), Sb element, CPC39820, WCB705/133, inner lateral view (IY127-029). *K,L*, Sc element; (*K*), CPC39821, WCB705/133, outer lateral view (IY126-008); (*L*), CPC39822, WCB705/133, outer lateral view (IY129-027). (*M*), Sd element, CPC39823, WCB705/133, inner lateral view (IY127-030). *N,O*, Pa element; (*N*), CPC39824, WCB705/243, inner lateral view (IY129-025); (*O*), CPC39825, WCB705/243, outer lateral view (IY129-026). (*P*), Pb element, CPC39826, WCB705/243, outer lateral view (IY129-006). Scale bars 100 μm.

van Wamel (1974), Lindström (in Ziegler, 1977), Stouge & Bagnoli (1999), Zhen *et al*. (2003), Nicoll & Ethington (2004) and Zhen *et al*. (2005). McTavish (1973) described *A. deltatus* and several other species of *Acodus* from the Emanuel Formation of the Canning Basin, and suggested a seximembrate apparatus for *A. deltatus* including prioniodiform (= P of our interpretation), ramiform (trichonodelliform = Sa, gothodiform = Sb, cordylodiform = Sc, and tetraprioniodiform = Sd of our interpretation), and oistodiform (= M of our interpretation) elements. Based on the stratigraphical distribution and morphological changes of various *Acodus* species recognized in the Emanuel Formation, McTavish (1973, fig. 7) indicated that both *Prioniodus* and *Baltoniodus* might have evolved from *Acodus*. Some authors went even further by attributing *A. deltatus* to either *Prioniodus* (van Wamel, 1974) or *Baltoniodus* (Bagnoli *et al*., 1988). In their revision of *A. deltatus*, Bagnoli *et al*. (1988) considered it to have a seximembrate apparatus without an Sa element, and included in this species some specimens from the Emanuel Formation illustrated by McTavish (1973). Subsequently Stouge & Bagnoli (1999) indicated that forms referred to *A. deltatus* by McTavish (1973), Ethington & Clark (1982) and

Repetski (1982) were actually species of *Diaphorodus* and not congeneric with their revised "*A*." *deltatus*.

Kennedy (1980) proposed *Diaphorodus* as the replacement of *Acodus* and selected *A. delicatus* Branson & Mehl, 1933 as the type species. In his revision of this species from the Early Ordovician Jefferson City Formation of Missouri, he recognized a seximembrate apparatus including the following types of elements: oistodiform (= M of our interpretation) represented by the form species *Oistodus expansus* Branson & Mehl, 1933 (see Kennedy, 1980, pl. 1, figs 20–22); acontiodiform (= Sa herein; see Kennedy, 1980, pl. 1, figs 14–17); drepanodiform (= ?Sc herein) represented by the form species *Cordylodus simplex* Branson & Mehl, 1933 (see Kennedy, 1980, pl. 1, figs 9–11); distacodiform (= Sd herein) represented by the form species *Paltodus distortus* Branson & Mehl, 1933 (see Kennedy, 1980, pl. 1, figs 18, 19); acodiform (= Pa herein) represented by the form species *A. delicatus* Branson & Mehl, 1933 (see Kennedy, 1980, pl. 1, fig. 3); and oistodiform (= ?Pb herein) represented by the form species *Oistodus vulgaris* Branson & Mehl, 1933 (see Kennedy, 1980, pl. 1, figs 23–25). This multi-element species reconstruction is more or less agreeable with our current understanding of *Acodus*, except that the asymmetrical tricostate Sb element was absent in the type species of *Diaphorodus* defined by Kennedy (1980). However, Stouge & Bagnoli (1999) considered both *Diaphorodus* and *Acodus* (represented by "*Acodus*" *deltatus*) as valid genera. According to their illustrations of both *Diaphorodus* sp. A from the Cow Head Group of western Newfoundland (Stouge & Bagnoli, 1999, pl. 1, figs 1–7) and "*A*." *deltatus* from the Köpingsklint Formation of Öland (Bagnoli *et al*., 1988; Stouge & Bagnoli, 1999, text-fig. 2), both *Diaphorodus* with a septimembrate apparatus and *Acodus* with a seximembrate apparatus have a nearly identical species apparatus and element morphology, except there is no Sa element for "*A*." *deltatus*. As argued by Zhen *et al*. (2005, p. 306), we prefer to retain *Acodus* as a valid genus and consider *Diaphorodus* tentatively as a junior synonym of *Acodus* pending further studies of these and other closely related forms.

Acodus deltatus? Linström, 1955

Fig. 4S–X

Acodus deltatus deltatus Linström.—McTavish, 1973: 39, pl. 1, figs 1–9, 12–14, text-fig. 3p–t.

Material. 209 specimens from three samples (Table 1).

Remarks. By assigning the Emanuel material to *Acodus deltatus* Lindström, 1955, McTavish (1973) defined *A. deltatus* as having a seximembrate apparatus. However, in a later revision of this Baltic species, Bagnoli *et al*. (1988) suggested that only some illustrated specimens referred to *A. deltatus deltatus* by McTavish (1973) might be doubtfully assignable to *A. deltatus*. Stouge & Bagnoli (1999) further indicated that the Emanuel material referred to *A. deltatus* was not conspecific with the type specimens from Sweden. As revision of the *Acodus* species described by McTavish (1973) and other related coniform taxa occurring in the Emanuel Formation is still in progress and will be presented elsewhere, the currently material is only tentatively referred to *A. deltatus*.

Acodus? transitans McTavish, 1973

Fig. 4M–R

Acodus transitans McTavish, 1973: 41, 42, pl. 1, figs 10, 11, 15, 17, 19, 21, 24, text-fig. 3 m–o.

Material. Four specimens from three samples WCB705/133 (Table 1).

Remarks. *Acodus transitans* is characterized by having a number of small and rudimentary denticles on the posterior process of its P and S elements, and represents a transitional form between *Acodus* and *Prioniodus*. Only a small number of specimens were available in this study (Fig. 4M–R). A comprehensive revision of *Acodus* species from the Emanuel Formation will be undertaken in a separate contribution.

Drepanodus Pander, 1856

Type species. *Drepanodus arcuatus* Pander, 1856.

Drepanodus arcuatus Pander, 1856

Fig. 5A–F

Drepanodus arcuatus Pander, 1856: 20, pl. 1, figs 2, 4–5, 17, 30, ?31; Löfgren & Tolmacheva, 2003: 211–215, figs 2, 3A–C, E–H, 5K–V, 6M–U, 7H–N, 8A–G (*cum syn*.); Zhen *et al*., 2004: 52–53, pl. 3, figs 1–12; Zhen *et al*., in press a: fig. 5A–N (*cum syn*.).

Material. 95 specimens from three samples (Table 1).

Remarks. Recently revised as having a septimembrate apparatus (Löfgren & Tolmacheva, 2003), *D. arcuatus* is a pandemic species widely distributed in various environments from inner shelf to slope (or basinal) settings with a long stratigraphic range from the late Tremadocian to Late Ordovician. It is a fairly common species in the Emanuel with specimens generally larger in comparison with those of other taxa. The cusp of the Sa element varies from proclined (Fig. 5B) to reclined (Fig. 5A), the Sd element has a twisted cusp and inwardly flexed anterobasal corner (Fig. 5C, D), the Pb element is characterized by having a strongly reclined cusp and a more or less square base in lateral view with basal margin curved into a right angle, and the Pa element bears a flared base with a shallower basal cavity (Fig. 5F). The symmetrical Sa element with a proclined cusp (Fig. 5B) is identical with the neotype and other illustrated specimens from western Russia and Sweden (Löfgren & Tolmacheva, 2003, fig. 3A, B, fig. 6O), and from the Honghuayuan Formation of Guizhou (Zhen *et al*., in press a, fig. 5B). The illustrated Sd, Pb and Pa elements are also comparable with those illustrated by Löfgren & Tolmacheva (2003) from Russia (fig. 3E–G) and Sweden (fig. 5O,V), and those from the Honghuayuan Formation of Guizhou (Zhen *et al*., in press a, fig. 5I, 5L, 5N).

Fig. 6. *A–F*, *Paracordylodus gracilis* Lindström, 1955. All from sample WCB705/243. (*A*), M element, CPC39827, anterior view (IY116-050). *B–E*, S elements; B–C, CPC39828, (*B*), inner lateral view (IY116-051); (*C*), close up showing chevron-shaped pattern of striae adjacent to anterior margin (IY126-052); (*D*), CPC39829, inner lateral view (IY126-053); (*E*), CPC39830, outer lateral view (IY126-054); (*F*), P element, CPC39928, outer lateral view (IY116055). *G,H,L*, *Prioniodus adami* Stouge & Bagnoli, 1988. G,H, Pa element, CPC39831, WCB705/243, (*G*), antero-outer lateral view (IY118-018); (*H*), outer lateral view (IY118-019). (*L*), Sa element, CPC39832, WCB705/243, posterior view (IY128-021). *M–R*, *Protoprioniodus simplicissimus* McTavish, 1973. All from sample WCB705/243. M, N, Sc element; (*M*), CPC39833, outer lateral view (IY118-020); (*N*), CPC39834, inner lateral view (IY118-030). *O,P*, Pa element, CPC39835, (*O*), inner lateral view (IY118-025); (*P*), upper-outer lateral view (IY118-023). *Q,R*, M element; (*Q*), CPC39836, anterior view (IY129-032); (*R*), CPC39837, posterior view (IY118-029). *I–K, S–V*, *Fahraeusodus adentatus* (McTavish, 1973). *I–K*, Sa element, CPC39838, WCB705/133, (*I*), lateral view (IY127-012); (*J*), anterior view, close up showing striae on the broad anterior face (IY127-011); (*K*), anterior view (IY127-010). (*S*), Sc element, CPC39839, 161–166 m, inner lateral view (IY130-001). (*T*), Sb element, CPC39840, 161–166 m, outer lateral view (IY130-002). *U,V*, Sd element, CPC39841, 161–166 m, (*U*), inner lateral view (IY130-005); (*V*), outer lateral view (IY130-006). Scale bars 100 μm unless otherwise indicated.

Drepanoistodus Lindström, 1971

Type species. *Oistodus forceps* Lindström, 1955.

Drepanoistodus sp. cf. *Drepanoistodus nowlani* Ji & Barnes, 1994

Fig. 5G–P

Drepanoistodus sp. cf. *Drepanoistodus nowlani* Ji & Barnes.—Zhen *et al*., 2007b: 132–134, pl. 2, figs 1–21, pl. 3, figs 1–9 (*cum syn.*).

Material. 52 specimens from three samples (Table 1).

Remarks. The Emanuel specimens are comparable with those described from the Honghuayuan Formation of Guizhou as *D*. sp. cf. *D. nowlani* except for the less extended basal-anterior corner in the P elements (Fig. 5N–P).

Fahraeusodus Stouge & Bagnoli, 1988

Type species. *?Microzarkodina adentata* McTavish, 1973.

Fahraeusodus adentatus (McTavish, 1973)

Fig. 6I–K, S–V

?Microzarkodina adentata McTavish, 1973: 49, 50, pl. 3, figs 28, 33–35, 38–40, 42–44.
Fahraeusodus adentatus (McTavish).—Stouge & Bagnoli, 1988: 119, pl. 4, figs 12–14 (*cum syn.*); Lehnert, 1995:89, pl. 7, fig. 20A, 20B.

Material. Seven specimens from two samples (Table 1).

Remarks. Specimens representing the asymmetrical Sb element with a lateral costa on the outer lateral face (Fig. 6T), the strongly asymmetrical Sc element without a lateral costa on each side (Fig. 6S), and the asymmetrical Sd element with a costa on each side (Fig. 6U, V) were recovered in the two samples from the Emanuel Formation. A specimen representing the triform Sa element with a broad, nearly flat anterior face and with a sharp anterolateral costa on each side (Fig. 6I–K) is also assigned to this species. McTavish (1973) recognized a quinquimembrate apparatus including oistodiform (= M element), ozarkodiniform (= P element), trichonodelliform (= Sa element), cordylodiform (= Sc element), and tetraprioniodiform (= Sd element), and doubtfully assigned it to *Microzarkodina*. Stouge & Bagnoli (1988) proposed *Fahraeusodus* and selected ?*M. adentata* as the type species. However, only a few specimens were recovered in the upper part of Bed 9 (*O. elegans* Biozone) of the Cow Head Group in Newfoundland, an interval stratigraphically slightly younger than the occurrence in the Emanuel Formation. The flat anterior face and edge-like anterolateral costa on each side of the Sa element are comparable with some specimens referred to *Fahraeusodus marathonensis* by Stouge & Bagnoli (1988, e.g., pl. 4, fig. 15) from the Cow Head Group.

Paracordylodus Lindström, 1955

Type species. *Paracordylodus gracilis* Lindström, 1955.

Paracordylodus gracilis Lindström, 1955

Fig. 6A–F

Oistodus gracilis Lindström, 1955: p. 576, pl. 5, figs 1–2.

Paracordylodus gracilis Lindström, 1955: p. 584, pl. 6, figs 11–12; Tolmacheva & Löfgren, 2000: 1117–1119, figs 5, 7; Tolmacheva & Purnell, 2002: 209–228, text-figs 1–10; Zhen *et al*., 2004: p. 56, pl. 4, figs 19–22 (*cum syn.*).

Material. 35 specimens from sample WCB705/243 (see Table 1).

Remarks. *Paracordylodus gracilis* is one of the best known species in the Early Ordovician. The reconstructed apparatus initially was based on interpretation of collections of discrete specimens documented successively by Sweet & Bergström (1972), McTavish (1973), and van Wamel (1974). Their collective interpretations were confirmed nearly 30 years later by the *in situ* bedding plane assemblages (Tolmacheva & Löfgren, 2000; Tolmacheva & Purnell, 2002). Its species composition and structure based on numerous clusters from deep water radiolarian cherts in central Kazakhstan revealed important data about its evolutionary affinities (Tolmacheva & Purnell, 2002). *Paracordylodus gracilis* is widely distributed (see Tolmacheva & Löfgren, 2000; Tolmacheva & Purnell, 2002), ranging from the late Tremadocian (late *P. proteus* Biozone) to late Floian (mid *O. evae* Biozone). It was most common in the Open Sea Realm (from shelf edge to basinal setting), with typical examples reported in central Kazakhstan (Tolmacheva & Purnell, 2002) occurring as the dominant species making up 90–99% of the specimen numbers. It is present in similar deep water oceanic settings in cherts of turbiditic successions (Percival *et al*., 2003), and also in allochthonous limestone or calcareous siltstone of slope settings (Zhen *et al*., 2004) in eastern Australia on the margins of eastern Gondwana. *Paracordylodus gracilis* was also common in the shallow marine environments within the Cold Domain of the Shallow-Sea Realm, such as in the Balto-Scandian Province (Löfgren, 1978; Tolmacheva & Löfgren, 2000). Its occasional presence in outer shelf environments or more rarely in inner shelf habitats within Temperate or even Tropical domains can be attributed to up-welling of cold ocean currents.

Paroistodus Lindström, 1971

Type species. *Oistodus parallelus* Pander, 1856.

Paroistodus parallelus (Pander, 1856) emend. Löfgren, 1997

Fig. 7A–S

Oistodus parallelus Pander, 1856: 27, pl. 2, fig. 40.
Paroistodus parallelus (Pander).—Lindström, 1971: 47, fig. 8; Löfgren, 1997: 923–926, pl. 1, figs 1–12, 17, 21, text-fig. 5A–G (*cum syn.*); Albanesi in Albanesi *et al*., 1998: 144, pl. 8, figs 27–30; Johnston & Barnes, 2000: 31–32, pl. 10, figs 10,11,15–17, 20; Tolmacheva *et al*., 2001: fig. 4.12–4.13; Viira *et al*., 2006: pl. 1, fig. 5.

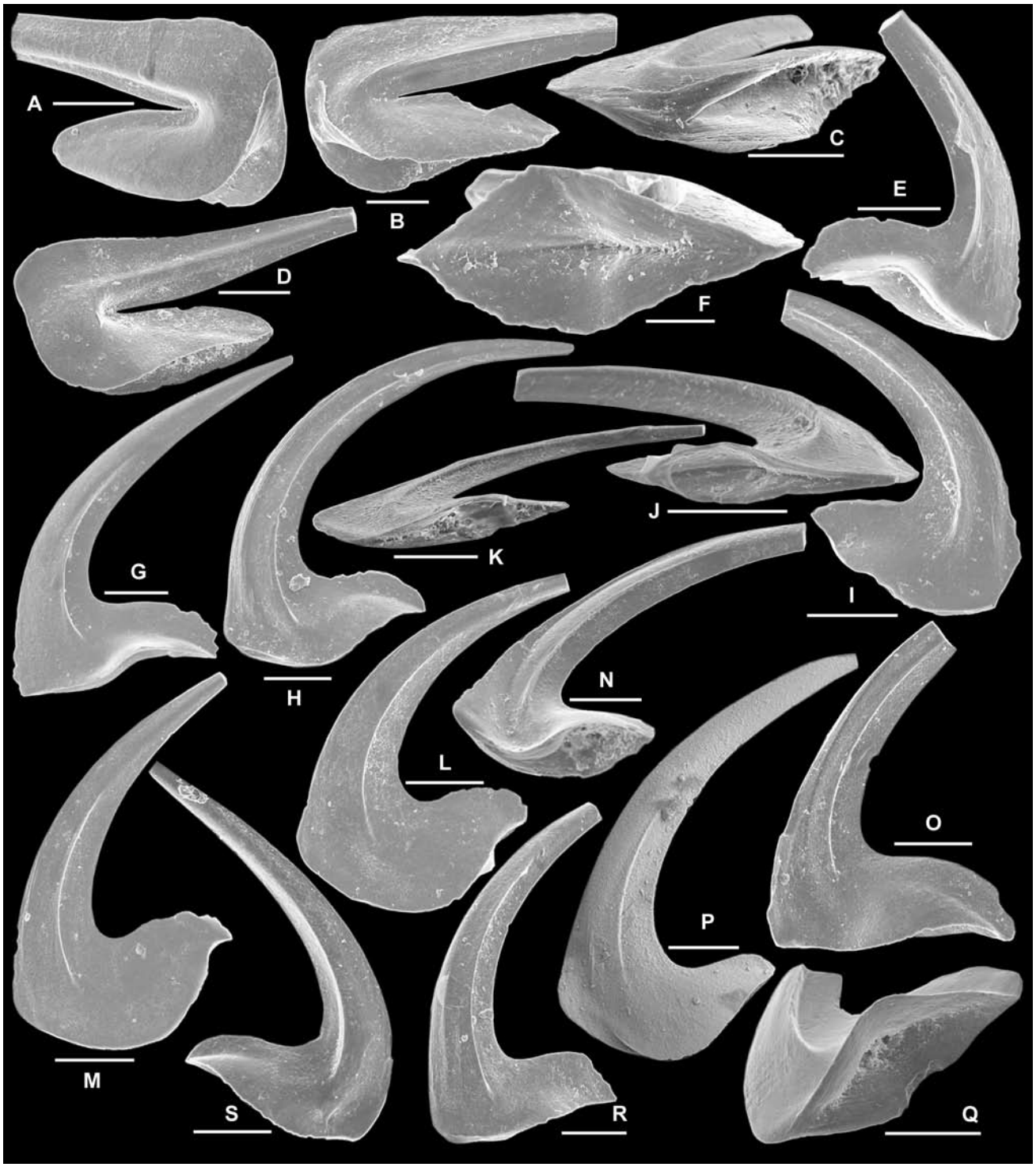

Fig. 7. *Paroistodus parallelus* (Pander, 1856). All from sample WCB705/133. *A–D*, M element; (*A*), CPC39842, anterior view (IY117-002); *B,C*, CPC39843, (*B*), anterior view (IY117-005); (*C*), basal view (IY117-006); (*D*), CPC39844, posterior view (IY117-008). *E–G*, Sa element; E,F, CPC39845, (*E*), lateral view (IY117-010), (*F*), basal view (IY117-011); (*G*), CPC39846, lateral view (IY117-009). *H–J*, Sb element; (*H*), CPC39847, outer lateral view (IY117-017); *I,J*, CPC39848, (*I*), inner lateral view (IY117-016), (*J*), basal view (IY117-018). *K–M*, Sc element; K,L, CPC39849, (*K*), basal view (IY117-014), (*L*), inner lateral view (IY117-013); (*M*), CPC39850, outer lateral view (IY117-012). *N,O*, Sd element; (*N*), CPC39851, inner-basal view (IY117-025); (*O*), CPC39852, outer lateral view (IY117-029). (*P*), Pb element; CPC39853, outer lateral view (IY132-020). *Q–S*, ?Pa element, (*Q*), CPC39854, basal view (IY117-036), (*R*), CPC39855, outer lateral view (IY117-030); (*S*), CPC39856, inner lateral view (IY117-034). Scale bars 100 μm.

Material. 457 specimens from three samples (Table 1).

Remarks. The species as revised by Löfgren (1997) possesses a septimembrate apparatus (including makellate M and drepanodiform or paroistodiform S and P elements), which can be distinguished from the other species of *Paroistodus* by having prominent lateral costae on the sides of its constituent elements. Zhen *et al*. (in press b) preferred to describe the S and P elements as paroistodiform in the *Paroistodus* species which show a sharp anterior costa extending basally into the basal cavity and forming a ridge-like structure (Zhen *et al*., 2007b, p. 137) at the anterior end of the basal cavity. However this character is not shown in the material of the two *Paroistodus* species (similar to *Paroistodus* sp. recently documented from the Honghuayuan Formation in South China) reported herein from the Emanuel Formation, although the anterior part of base often exhibits a zone of recessive basal margin (Figs 7A–C, 8H). *Paroistodus parallelus* occurs abundantly in the Emanuel Formation, where it is found in association with *P. proteus* although the latter is rare (Table 1).

Paroistodus proteus (Lindström, 1955) emend. Löfgren, 1997

Fig. 8A–K

Drepanodus proteus Lindström, 1955: 566, pl. 3, figs 18–21, text-fig. 2a–f, j.
Paroistodus proteus (Lindström).—Löfgren, 1997: 922–923, text-figs 3H–N, 4L–AB (*cum syn.*); Zhen *et al*., 2007b: 136, 137, pl. 5, figs 1–11 (*cum syn.*).

Material. 30 specimens from three samples (Table 1).

Remarks. *Paroistodus parallelus* is relatively rare in the Emanuel samples, and can be easily differentiated from associated *P. parallelus* mainly by lacking a prominent costa on the lateral faces. *Paroistodus proteus* was revised by Löfgren (1997) as having a septimembrate apparatus. After a review of previously reported occurrences of this species in the Honghuayuan Formation and other coeval stratigraphic units in South China and comparison with Baltic material of *P. proteus*, Zhen *et al*. (2007b) concluded that *Paroistodus* is represented in the Honghuayuan Formation by a rare form that they identified as *Paroistodus* sp. It differs from *P. proteus* in having a smooth lateral face without a carina and having a more open basal cavity which lacks the distinctive so-called paroistodiform character. The material from the Emanuel Formation is transitional between typical *P. proteus* from the late Tremadocian to Floian of Balto-Scandia and *Paroistodus* sp. from the Honghuayuan Formation of South China. It is comparable with *P. proteus* in having a prominent carina (Fig. 8A–E) or even a weak costa (Fig. 8J) on the lateral faces, but similar to *Paroistodus* sp. from the Honghuayuan Formation in lack of the paroistodiform feature. As mentioned above, absence of the paroistodiform character in species of *Paroistodus* co-occurring in the Emanuel Formation may indicate that this feature is caused by ecological adaption rather than as a phylogenetically significant trait for *Paroistodus*. Interestingly, *P. proteus* from the Emanuel Formation of Western Australia and from the Latorp Limestone and Tøyen Shale of Sweden and *Paroistodus* sp. from the Honghuayuan Formation of South China come from three contrasting ecological/sedimentological settings; they may represent three populations or subspecies of *P. proteus*. The typical latest Tremadocian and early Floian *P. proteus*-bearing successions in Sweden (e.g., Diabasbrottet area) were deposited in the outer shelf settings of the Cold Domain (Bergström *et al*., 2004), and the mid-upper part of the Emanuel Formation might be largely deposited in deep subtidal settings, while the Honghuayuan Formation with *Paroistodus* sp. apparently represents typical shallow subtidal environments. Therefore, in consideration of the relationship between their morphological variation and their ecological/geographical distributions, the material from the Emanuel Formation is considered as conspecific with type material of *P. proteus*, and *Paroistodus* sp. from the Honghuayuan Formation (Zhen *et al*., 2007b) might be better treated as a separate subspecies of *P. proteus*.

Prioniodus Pander, 1856

Type species. *Prioniodus elegans* Pander, 1856.

Prioniodus adami Stouge & Bagnoli, 1988

Fig. 6G–L

Prioniodus sp. nov. C McTavish, 1973: 47, pl. 3, figs 4–6, ?11, 16, text-fig. 6f, g, i, ?j, k.
Prioniodus adami Stouge & Bagnoli, 1988: 132, 133, pl. 11, figs 5–13 (*cum syn.*); ?Albanesi *et al*., 1998: 155, pl. 10, figs 1–3; Johnston & Barnes, 2000: 36, pl. 16, figs 9, 10, 13–16, 19; Pyle & Barnes, 2002: 110, pl. 26, figs 19–21.

Material. Four specimens from two samples (Table 1).

Remarks. Based on a large collection from Bed 9 of the Cow Head Group of western Newfoundland, Stouge & Bagnoli (1988) established *P. adami* as having a septimembrate apparatus (pastinate Pa, and Pb, ramiform S and geniculate M elements), and also included in it the material from the Emanuel Formation that McTavish (1973), ascribed to *Prioniodus* sp. C except for the oistodiform element (his pl. 3, fig. 11, text-fig. 6j) which bears a short, adenticulate inner lateral process. *Prioniodus adami* is characterized by bearing small, closely-spaced denticles on the long posterior process of the S and P elements, as well as on the anterior and outer lateral processes of the P elements and the inner lateral process of the M element. The Pa element (Fig. 6G, H) from the Emanuel Formation is identical with those illustrated by McTavish (1973, pl. 3, figs 5, ?16), but exhibits less closely spaced denticles on the processes in comparison with the holotype (Stouge & Bagnoli, 1988, pl. 11, fig. 8). The M element from the Cow Head Group shows a long adenticulate outer lateral process and a long, denticulate inner lateral process with small, closely-spaced denticles, similar to those on the processes of the P and S elements, but no M element has been recovered from the samples of this study.

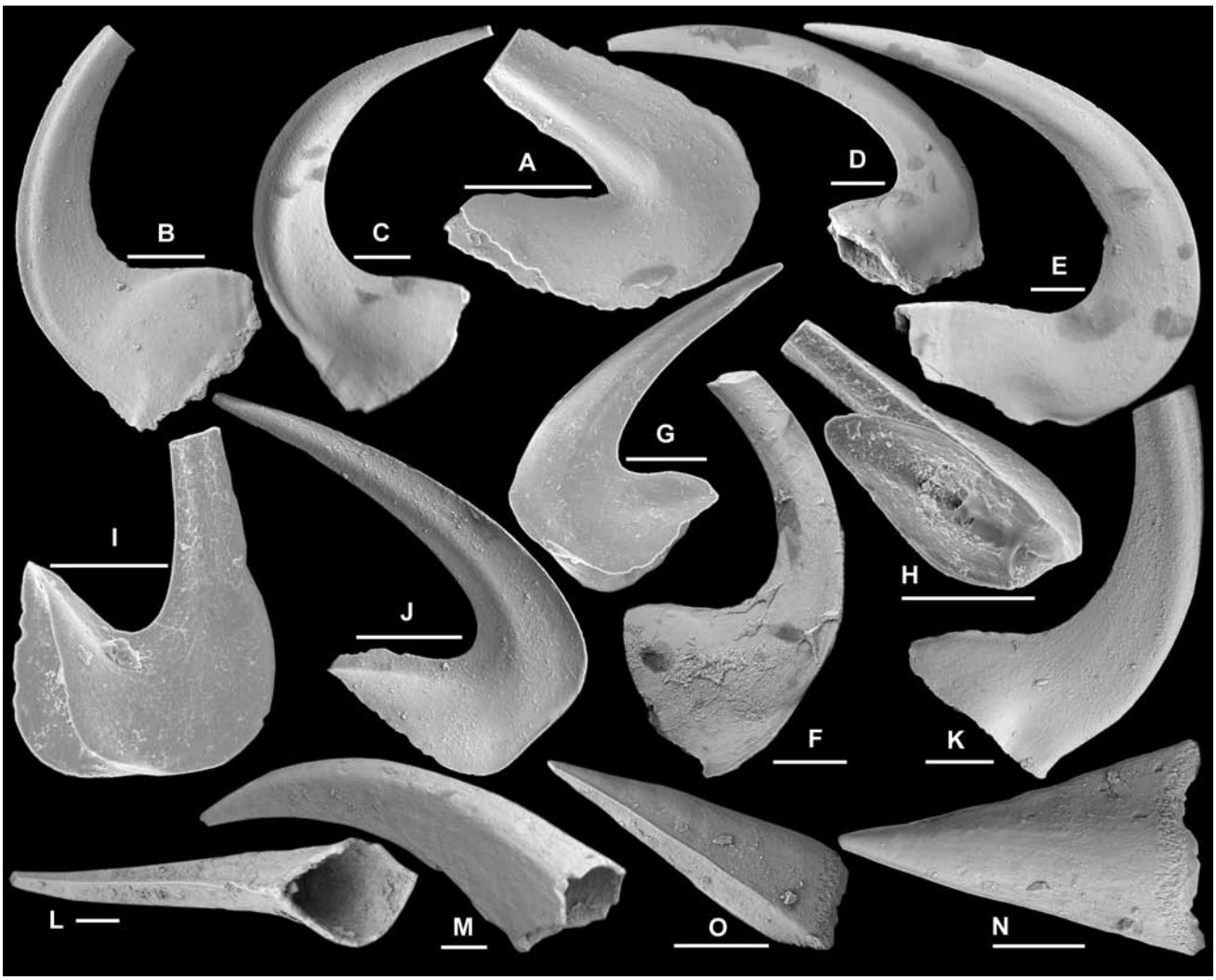

Fig. 8. *A–K*, *Paroistodus proteus* (Lindström, 1955). (*A*), M element, CPC39857, WCB705/133, posterior view (IY132-023). *B,C*, Sb element; (*B*), CPC39858, WCB705/133, inner view (IY132-022); (*C*), CPC39859, WCB705/133, outer lateral view (IY130-040). *D,E*, Sc element; (*D*), CPC39860, 161–166m, outer lateral view (IY130-025); (*E*), CPC39861, WCB705/133, inner lateral view (IY132-029). (*F*), Sd element, CPC39862, 161–166m, innrt lateral view (IY130-026). *G–J*, Pb element; (*G*), CPC39863, WCB705/133, outer lateral view (IY117-020); *H,I*, CPC39864, WCB705/133, (*H*), basal view (IY117-021), (*I*), inner lateral view (IY117-022); (*J*), CPC39865, WCB705/133, inner lateral view (IY130-043). (*K*), Sa element, CPC39866, WCB705/133, lateral view (IY130-41). *L–O*, gen. et sp. indet. A. All from sample WCB705/133. *L,M*, symmetrical element, CPC39867, (*L*), basal-posterior view (IY132-024), (*M*), lateral view (IY132-025). *N,O*, asymmetrical element, CPC39868, (*N*), outer lateral view (IY132-028), (*O*), anterior view (IY132-027). Scale bars 100 μm.

Protopanderodus Lindström, 1971

Type species. *Acontiodus rectus* Lindström, 1955.

Protopanderodus gradatus Serpagli, 1974

Fig. 9A–P

Protopanderodus gradatus Serpagli, 1974: 75, pl. 15, figs 5a–8b, pl. 26, figs 11–15, pl. 30, figs 1a–b; text-fig. 17; Zhen *et al*., 2004: 56–57, pl. 5, figs 1–10 (*cum syn.*); Zhen & Percival, 2006: fig. 9A–C; Zhen *et al*., in press a: fig. 8A–Q.

Material. 126 specimens from two samples (Table 1).

Remarks. *Protopanderodus gradatus* is common in one (WCB705/243) of the samples studied from the Emanuel Formation. This material is identical with the types described from the San Juan Formation (Early Ordovician) of Argentine Precordillera (Serpagli, 1974), and those recently documented from the Honghuayuan Formation of Guizhou, South China (Zhen *et al*., in press a, fig. 8A–Q). An additional element (Fig. 9J–P) bearing a more compressed cusp and a less extended base with a rounded basal margin has also been recognized in the Emanuel material. It also shows rather prominent striation in the area immediately anterior to the lateral costa, and a weakly developed chevron-shaped pattern of striae adjacent to the anterior margin (Fig. 9K, O). As these distinctive characters are not observed in the other elements of *P. gradatus*, it is tentatively assigned herein to the M position of *P. gradatus*. Some specimens bear rounded holes of about 3–4.5 μm in diameter, presumably representing the boring structure made by an unknown organism (Fig. 9O, P).

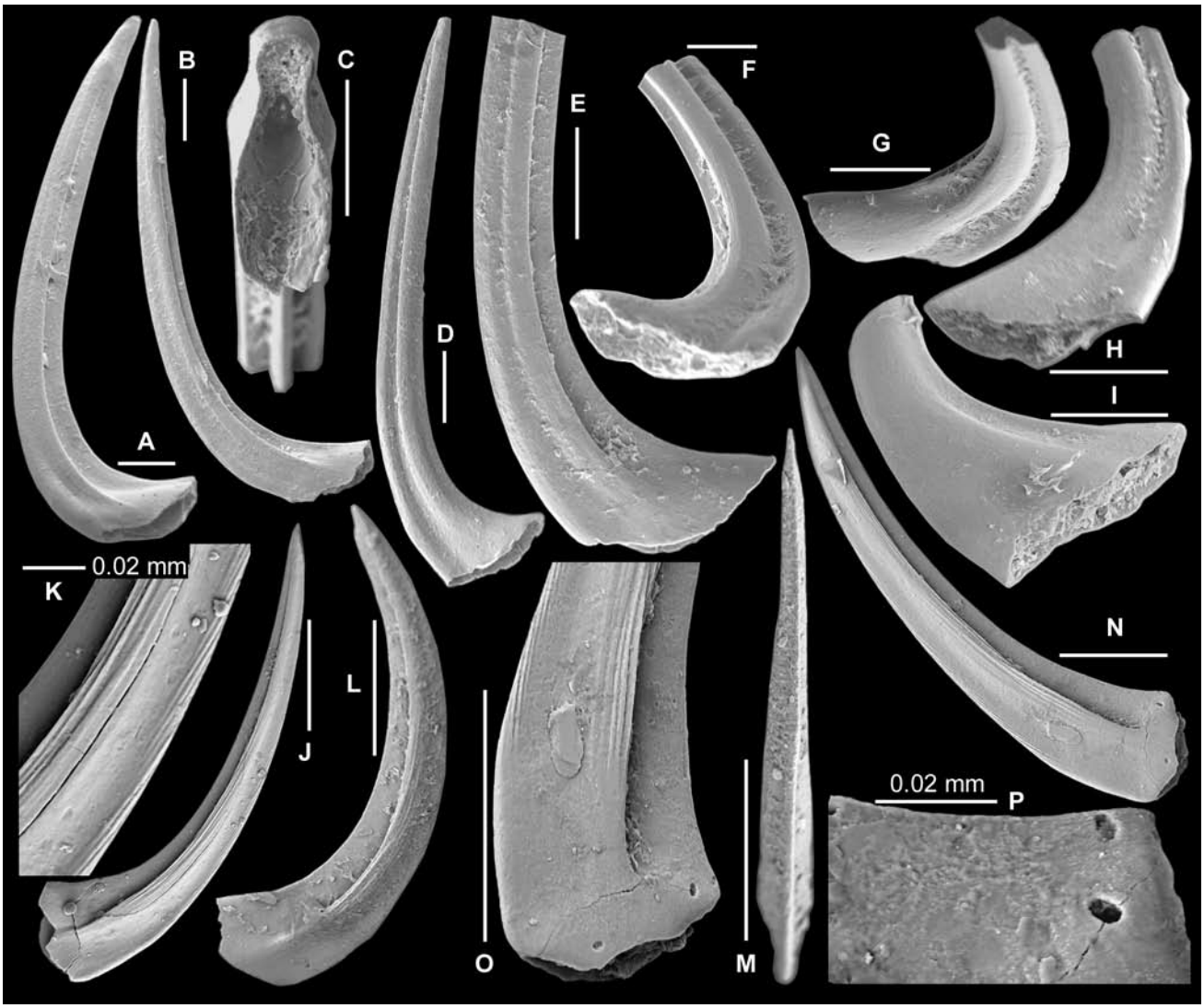

Fig. 9. *Protopanderodus gradatus* Serpagli, 1974. All from sample WCB705/243. *A–C*, Sa element; (*A*), CPC39869, lateral view (IY128-010); (*B*), CPC39870, lateral view (IY128-011); (*C*), CPC39871, basal view (IY128-008). *D–G*, Sc element; (*D*), CPC39872, inner lateral view (IY128-001); (*E*), CPC39873, inner lateral view (IY128-002); (*F*), CPC39874, basal-inner lateral view (IY128-005); (*G*), CPC39875, upper-inner lateral view (IY128-009). *H,I*, P element, CPC39876, (*H*), inner lateral view (IY128-019); (*I*), basal-outer lateral view (IY128-020). *J–P*, ?M element; J–K, CPC39877, (*J*), inner lateral view (IY129-037); (*K*), close-up inner lateral view, showing striae near the furrow and chevron-shaped pattern of striae adjacent to anterior margin (IY129-038); *L,M*, CPC39878, (*L*), outer lateral view (IY129-041); (*M*), anterior view (IY129-039); *N–P*, CPC39879, (*N*), inner lateral view (IY129-042); (*O*), close-up inner lateral view, showing striae near the furrow and chevron-shaped pattern of striae adjacent to anterior margin (IY129-043); (*P*), close up showing rounded boring hole on the surface (IY129-044). Scale bars 100 μm unless otherwise indicated.

Scolopodus Pander, 1856

Type species. *Scolopodus sublaevis* Pander, 1856.

Scolopodus houlianzhaiensis An & Xu in An *et al.*, 1983

Fig. 10A–K

Scolopodus rex houlianzhaiensis An & Xu in An *et al*., 1983: 148, pl. 12, figs 23–27, text-fig. 11.7, 11.8; ?Ding, 1987: pl. 6, fig. 23; non Ding *et al*. in Wang, 1993: 205, pl. 14, figs 13–15.

Scolopodus houlianzhaiensis An & Xu.—Zhen *et al*., in press a: fig. 9G–L.

Material. 19 specimens from three samples (Table 1).

Remarks. The multicostate Sa (symmetrical) and Sb (asymmetrical) elements of *Scolopodus houlianzhaiensis* show some resemblance to *S. quadratus*, but the distinctive Sc element has a strongly compressed cusp and lateral costae restricted to near the anterior margin (Fig. 10J, K). An & Xu (in An *et al*., 1983) considered this species as a subspecies of *Scolopodus rex* Lindström, 1955, which is now regarded as a junior synonym of *Scolopodus striatus* Pander, 1856 (see Fåhraeus, 1982, Zhen *et al*., 2004; Tolmacheva, 2006).

An & Xu (in An *et al*., 1983) suggested a bimembrate apparatus including symmetrical and asymmetrical elements. Three morphotypes, representing symmetrical multicostate Sa, asymmetrical multicostate Sb, and strongly asymmetrical Sc elements, can be recognized among our Emanuel material. The Sa element (Fig. 10A–D) has a broad anterior face, five or six sharp costae on each side and a costa along the posterior margin, and is identical with the symmetrical element defined by An *et al*. (1983, pl. 12, figs 23–25) from the Liangjiashan Formation of North China. The Sb element

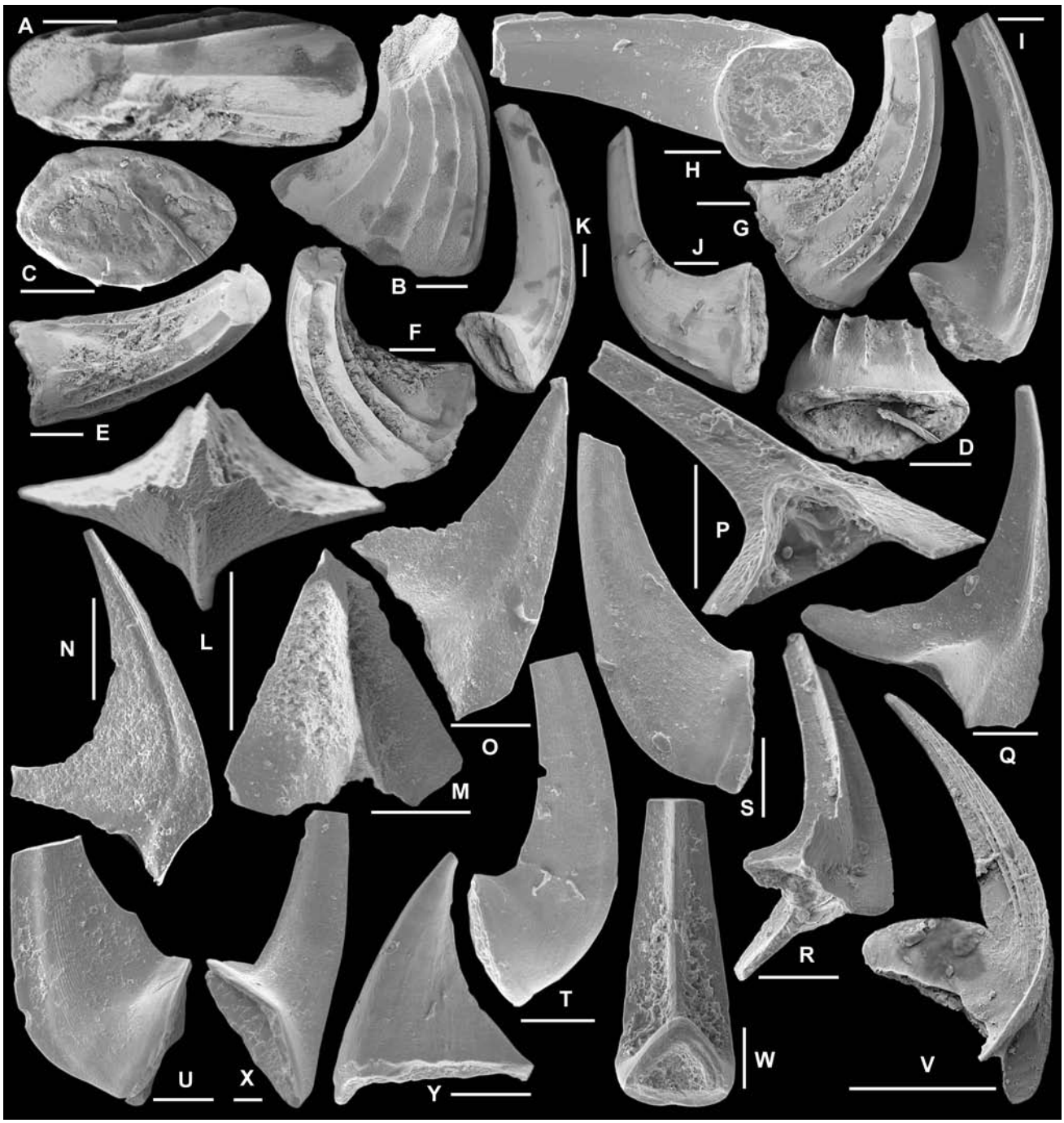

Fig. 10. *A–K*, *Scolopodus houlianzhaiensis* An & Xu in An *et al*., 1983. All from sample 161–166 m. *A–D*, Sa element; *A,B*, CPC39880, (*A*), posterior view (IY130-011), (*B*), lateral view (IY130-010); *C,D*, CPC39881, (*C*), basal view (IY130-009), (*D*), lateral view (IY130-007). *E–G*, Sb element, CPC39882, (*E*), posterior view (IY130-017), (*F*), inner lateral view (IY130-016), (*G*), outer lateral view (IY130-018). *H–K*, Sc element; H,I, CPC39883, (*H*), posterior view (IY129-028), (*I*), inner lateral view (IY129-029); *J,K*, CPC39884, (*J*), outer lateral view (IY130-019), (*K*), inner lateral view (IY130-021). *L–R*, *Lissoepikodus nudus* Nicoll & Ethington, 2004. *L,M*, Sa element, CPC39885, WCB705/133, (*L*), upper view (IY127-002); (*M*), posterior view (IY127-003). *N,O*, Pb element; (*N*), CPC39886, WCB705/133, outer lateral view (IY127-014); (*O*), CPC39887, WCB705/133, outer lateral view showing weaker costa (IY127-006). *P,Q*, Sb element; (*P*), CPC39888, WCB705/243, basal view (IY118-016); (*Q*), CPC39889, WCB705/133, inner lateral view (IY126-034). (*R*), Sd element, CPC39890, WCB705/133, basal-inner lateral view (IY126-033). *S–U*, *Nasusgnathus dolonus* (An, 1981). All from sample WCB705/133. *S,T*, Sd element; (*S*), CPC39891, inner lateral view (IY127-008); (*T*), CPC39892, outer lateral view (IY127-007). (*U*), Sb element, CPC39893, WCB705/133, outer lateral view (IY127-005). (*V*), ?*Protoprioniodus simplicissimus* McTavish, 1973. Sb element, CPC39894, WCB705/243, outer lateral view (IY129-035). (*W*), gen. et sp. indet. B. Sa element, CPC39895, WCB705/133, posterior view (IY126-036). (*X*), *Paltodus* sp. M element, CPC39896, WCB705/133, posterior view (IY126-014). (*Y*), gen. et sp. indet. A. Symmetrical stout element, CPC39897, WCB705/133, lateral view (IY127-034). Scale bars 100 μm unless otherwise indicated.

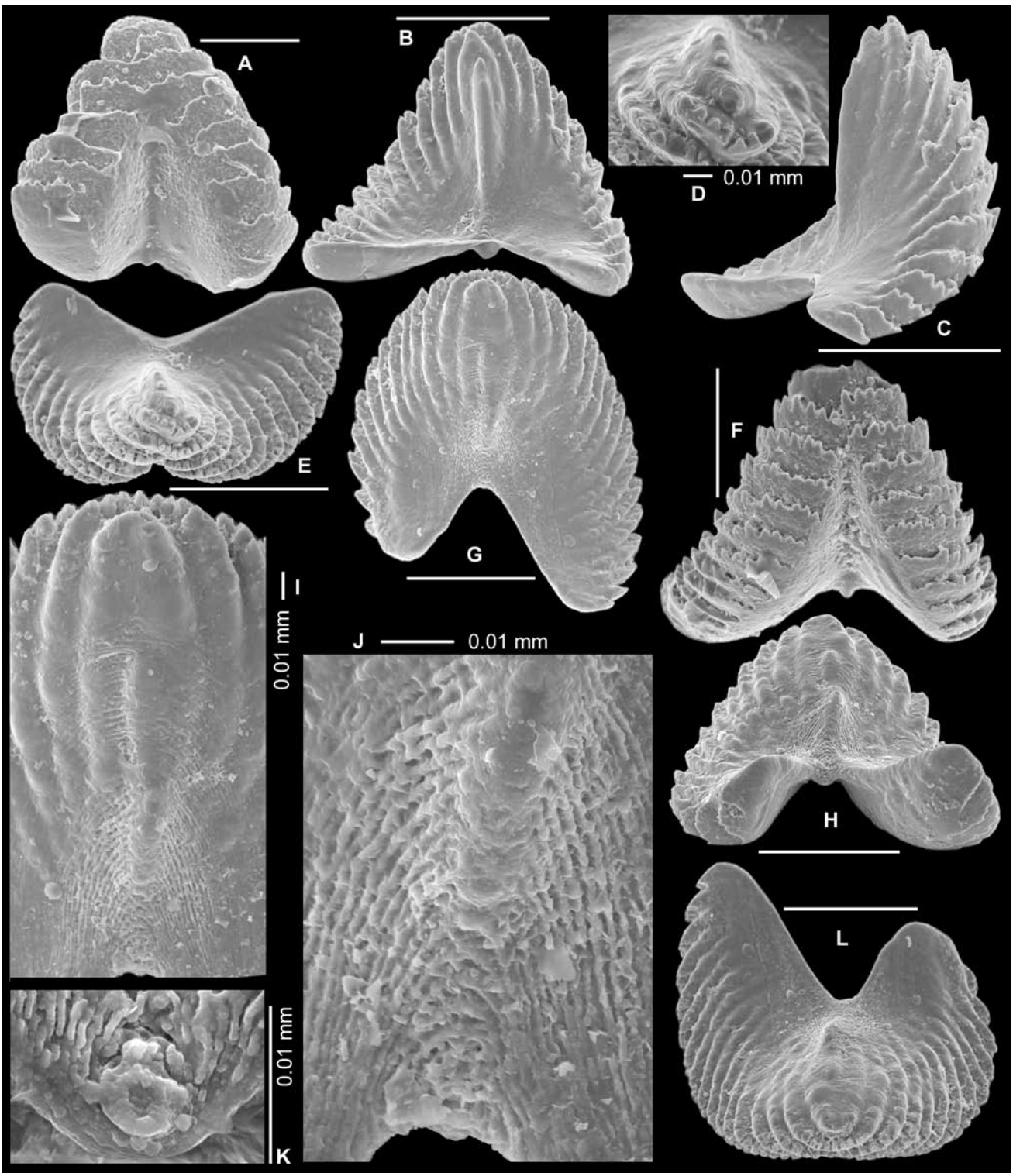

Fig. 11. *Serratognathus bilobatus* Lee, 1970. (*A*), Sa element, CPC39898, 161–166 m, anterior view (IY116-041). *B–F*, Sb element; *B–E*, CPC39899, WCB705/133, (*B*), posterior view (IY116-002), (*C*), outer lateral view (IY116-006), (*D*), upper view showing the tip of the cusp (IY116-012), (*E*), upper view (IY116-011); (*F*), CPC39900, WCB705/133, anterior view (IY116-028). *G–L*, Sc element, CPC39901, WCB705/133, (*G*), posterior view (IY116-013), L, upper view (IY116-023), (*H*), basal-posterior view (IY116018), (*I*), posterior view of the cusp (IY116-014), (*J*), posterior view, close up showing fine striae (IY116-015), (*K*), basal view showing ring-like basal node (IY116-022). Scale bars 100 μm unless otherwise indicated.

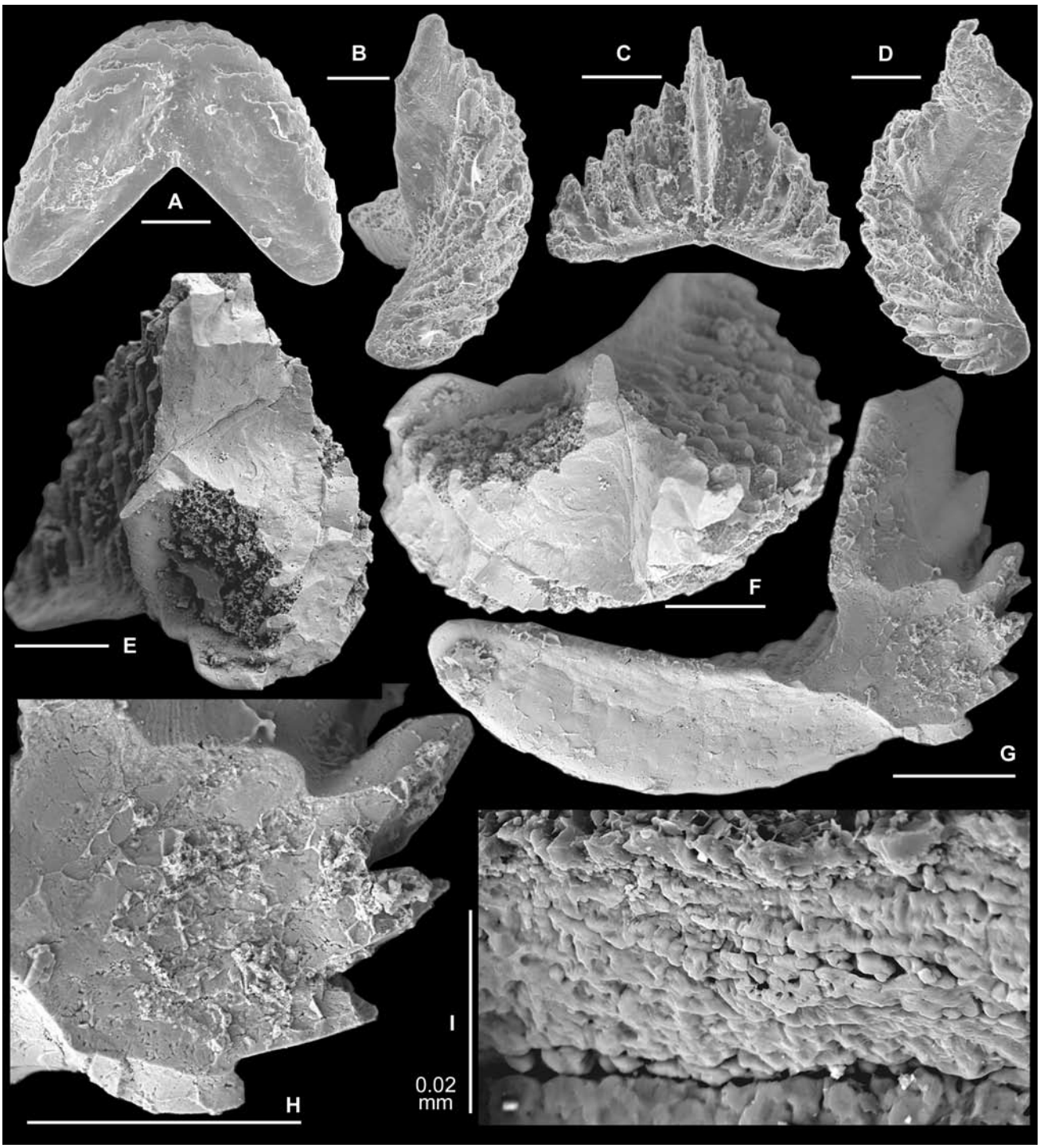

Fig. 12. *Serratognathus diversus* An, 1981. All from the Honghuayuan Formation in Guizhou. *A–C*, Sa element; (*A*), AM F.135048, THH7, anterobasal view (IY119-004); (*B*), AM F.135044, THH7, lateral view (IY119-002); (*C*), AM F.135047, THH10, posterior view (IY119-040). (*D*), Sb element, AM F.135049, THH7, outer lateral view (IY119014); *E–H*, broken specimens showing overlapping laminar layers on the surface of breakage. *E,F*, Sb element, AM F.135815, THH7, (*E*), postro-lateral view (IY133-035), (*F*), upper view (IY133-037); *G,H*, Sc element, AM F.135816, THH9, (*G*), inner lateral view (IY133-040), (*H*), close up showing the surface of breakage (IY133-041); (*I*), Sc element, AM F.135817, YTH10, showing the partition between laminar layers and the fine laminar structure within each laminar layer (IY133-033). Scale bars 100 μm unless otherwise indicated.

[Fig. 13 caption continued]… *G,H*, Sb element, AM F.135823, WHC36, (*G*), antero-outer lateral view, bearing 10 laminar layers (IY133-013), (*H*), close up showing denticles along anterior margin of each laminar layer (IY133-014). *I,J*, Sc element, AM F.135824, WHC36, (*I*), antero-outer lateral view, bearing 17 laminar layers (IY133-006), (*J*), posterior view (IY134-001). *K, L*, Sc element, AM F.135825, THH12, (*K*), anterior view, bearing 20 laminar layers (IY133-044), (*L*), posterior view (IY134-029). (*N*), Sc element, AM F.135826, WHC35, close up showing the small ring-like node representing the initial stage of the element (IY134-014). (*O*), Sc element, AM F.135817 (same specimen as Fig. 12I), YTH10, close up showing the rounded pit-like initial stage of the element (IY133-028). Scale bars 100 μm, unless indicated otherwise.

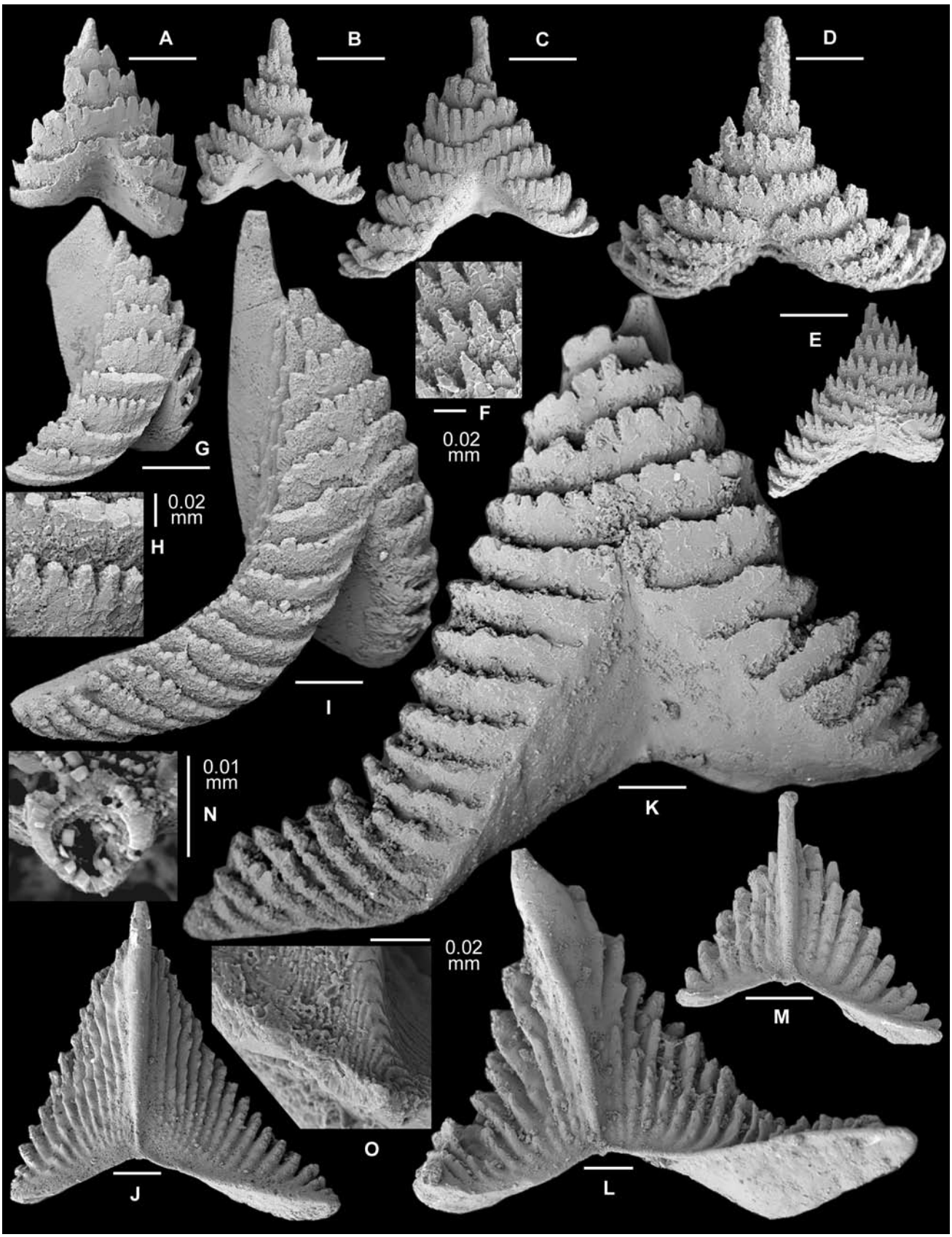

Fig. 13. *Serratognathus diversus* An, 1981. All from the Honghuayuan Formation in Guizhou. Showing size variation; A–*E,G,I,K* and *M* are magnified equally. (*A*), Sb element, AM F.135818, AFI983A, anterior view, bearing six laminar layers (IY133-046). (*B*), Sb element, AM F.135819, THH10, anterior view, bearing six laminar layers (IY133-038). *C,M*, Sc element, AM F.135820, YTH5, (*C*), anterior view, bearing eight laminar layers (IY133-024), (*M*), posterior view (IY134-019). (*D*), Sa element, AM F.135821, AFI986, upper-anterior view, bearing eight laminar layers (IY133-050). *E,F*, Sc element, AM F.135822, YTH4, (*E*), anterior view, bearing 10 laminar layers (IY133-021), (*F*), close up showing denticles along anterior margin of each laminar layer (IY133-022). …[continued on facing page]

resembles the Sa, but is asymmetrical with a more convex outer lateral face (Fig. 10E–G). The Sc element is identical with the asymmetrical element represented by the holotype of the species from the Liangjiashan Formation of North China (An *et al*., 1983, pl. 12, fig. 26) with a convex outer lateral face and concave inner lateral face and with several costae (2 to 4) near the anterior margin (Fig. 10H–K). Zhen *et al*. (in press a, fig. 9G–L) reported the occurrence of this species in the Honghuayuan Formation in Guizhou. The Sc element recently illustrated from the Honghuayuan Formation in Guizhou (Zhen *et al*., in press a, fig. 9G–I) shows a more compressed base, and the Sa element (Zhen *et al*., in press a, fig. 9J–L) has the base less extended posteriorly, with costae on the lateral face more towards anterior.

Semiacontiodus Miller, 1969

Type species. *Semiacontiodus nogamii* Miller, 1969.

Semiacontiodus sp. cf. *Semiacontiodus cornuformis* (Sergeeva, 1963)

Fig. 15L–T

Scolopodus cornuformis Sergeeva.—An, 1987: 183, pl. 7, figs 10–11, 13–16; Ding *et al*. in Wang, 1993: 202, pl. 5, fig. 33; Zhen *et al*., in press a: fig. 9D–F.

Material. 26 specimens from three samples (Table1).

Remarks. Three morphotypes of this species are recognized in the Emanuel samples representing a symmetry transition series including symmetrical Sa (Fig. 15L,M), asymmetrical Sb (Fig. 15N,O), and strongly asymmetrical and laterally more compressed Sc (Fig. 15P–T) elements. Although these specimens have relatively shorter bases, they otherwise resemble those of *S. cornuformis* (Sergeeva, 1963), which was revised as consisting of a septimembrate apparatus (Löfgren, 1999).

Serratognathus Lee, 1970

Type species. *Serratognathus bilobatus* Lee, 1970.

Serratognathus bilobatus Lee, 1970

Fig. 11A–L

Serratognathus bilobatus Lee, 1970: 336, pl. 8, figs 6, 7; Metcalfe, 1980: pl. 1, figs 16–19; An, 1981: pl. 2, fig. 26; An & Ding, 1982: pl. 5, fig. 25; An *et al*., 1983: 149, pl. 16, figs 20–22, pl. 17, figs 1, 2; An, 1987: 189, 190, pl. 18, fig. 11; Ding, 1987: pl. 6, fig. 16; An & Zheng, 1990: pl. 7, fig. 13; Ding *et al*. in Wang, 1993: 207, pl. 20, fig. 5; Chen & Wang, 1993: fig. 2Q, 2U; Wang *et al*., 1996: pl. 2, figs 1–7, 9; Nicoll & Metcalfe, 2001: fig. 6.19–6.22; Metcalfe, 2004: pl. 2, figs 9–10.

Material. Seven specimens from three samples (Table 1).

Diagnosis. Species of *Serratognathus* with a trimembrate apparatus, including symmetrical Sa, asymmetrical Sb, and strongly asymmetrical Sc elements; all elements semi-conical in outline with fan-shaped array of small, closely spaced denticles along anterior and lateral edges of overlapping laminar layers; cusp small, posteriorly positioned and anterolaterally enclosed by up to 16 vertically overlapping laminar layers, which are anterobasally divided by a broad median groove into two lobe-like lateral processes; basal cavity absent.

Description. Trimembrate apparatus, including symmetrical Sa, asymmetrical Sb, and strongly asymmetrical Sc elements which form a symmetry transition series; each element semi-conical in outline, formed by upwardly overlapping layers, resembling a half-cut onion; composed of the cusp and a gently posterolaterally extended lobe-like lateral process on each side. Cusp small or indistinctive, weakly compressed laterally with a broad posterior face, and the anterior margin embedded in up to 16 surrounding overlapping layers, which are bordered by small, closely spaced denticles along the anterior and lateral margins. Discrete denticles surround the cusp in a semicircle, representing the anterolateral edge of each overlapping layer. Node-like denticles weakly developed on posterior face, may be absent towards the base (Fig. 11B, E, G, I); fine striae microstructure best developed on the posterior face in the area above the basal margin (Fig. 11 I, J). Denticulate anterior margin of each layer turned upwards. Basal face smooth, wide, and distally arched; crescentic in outline in basal view; bisected by anteroposteriorly directed median groove extending anterobasally to separate into two lobes underneath each lateral process. Basal cavity absent; basal end of the cusp represented by a small ring-like node (Fig. 11K), but in one specimen basal cavity represented by a small, shallow pit underneath the cusp (Fig. 11B).

Sa element symmetrical, outline crescentic in upper view with convex anterior face and concave posterior face, and tower-like in anterior view (Fig. 11A). Cusp small, located posteromedially with a short lobe-like process on each side, which extends posterolaterally; in anterior view, two processes separated anterobasally by a prominent rather deep median groove (Fig. 11A). Basal face smooth, bisected by the median groove into two symmetrical lobes.

Sb element (Fig. 11B–F) like Sa, but asymmetrical; inner lateral process shorter in posterior view (Fig. 11B), extending laterally with basal margin nearly horizontal; outer lateral process longer extending posterolaterally (Fig. 11C). Basal margin of the two processes forming an angle of 125° or more in the upper view (Fig. 11E). Basal face asymmetrical, with a longer lobe under outer lateral process and a shorter lobe under inner lateral process. One specimen (Fig. 11B) exhibits a small and shallow basal cavity.

Sc element (Fig. 11G–L) similar to Sb, but strongly asymmetrical with longer and more strongly posteriorly extended lateral processes. In upper view, the basal margins of the two lateral processes form a rather narrower angle of about 70–80° (Fig. 11G, L); outer lateral process longer (Fig. 11G, L).

Remarks. Lee (1970) illustrated two specimens of *Serratognathus bilobatus* from the Dumugol Formation of South Korea, with the figured holotype (Lee, 1970, pl. 8, fig. 7a–d) assignable to the asymmetrical Sb element defined herein and the other figured paratype (Lee, 1970, pl. 8, fig. 6) is a symmetrical Sa element. Both specimens are identical with those from the Emanuel Formation. *Serratognathus bilobatus* differs from *S. diversus* An, 1981 (Figs 12–14) from the Honghuayuan Formation of South China mainly in having a smaller, often indistinct, cusp (Fig. 11G, H).

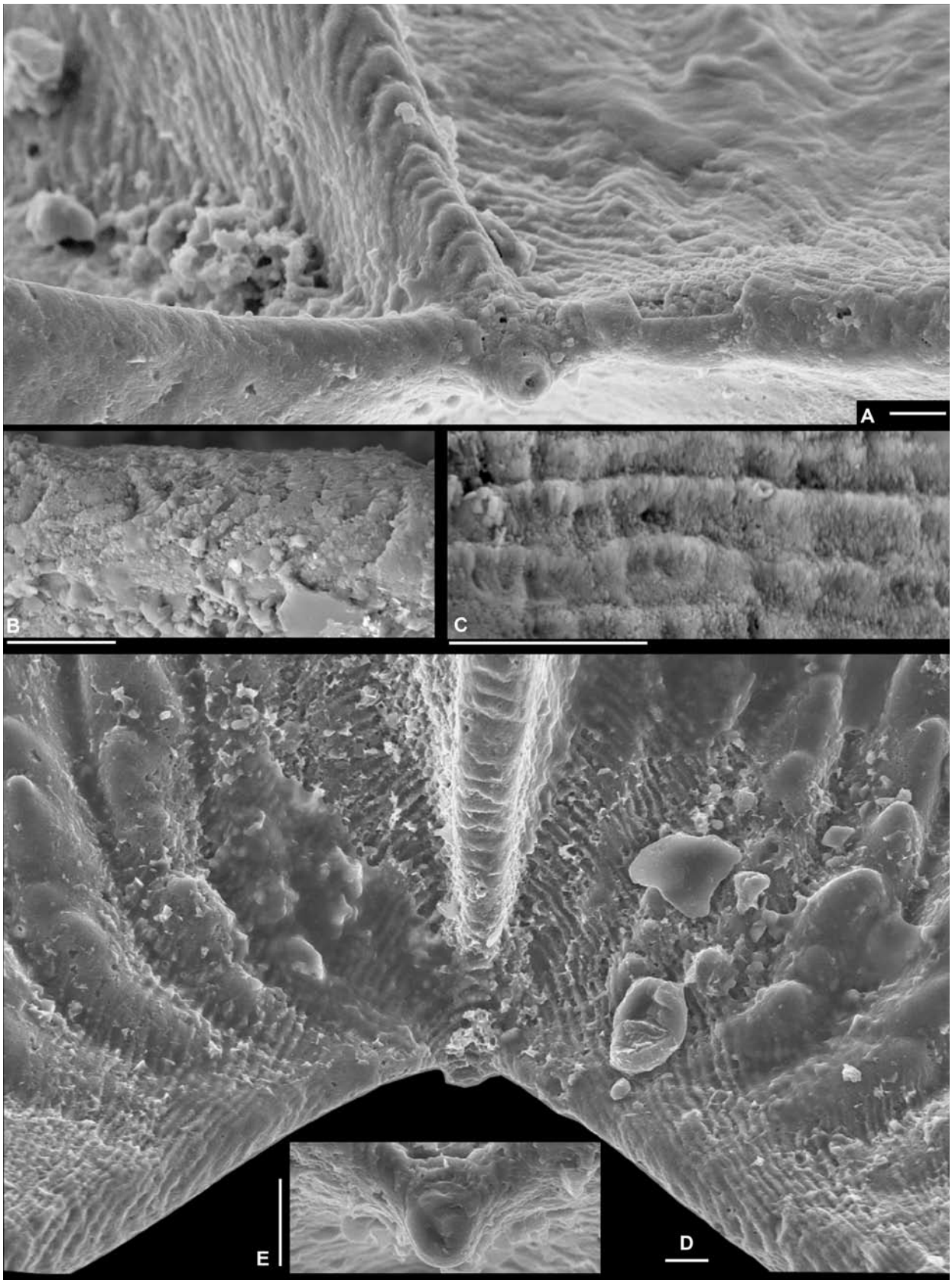

Fig. 14. *Serratognathus diversus* An, 1981. All from the Honghuayuan Formation in Guizhou. (*A*), Sb element, AM F.135050, THH7, basal-posterior view, showing fine growth laminar preserved on the lateral and posterior surfaces of the cusp (IY119-022). (*B*), Sc element, AM F.135825 (same specimen as Fig. 13K,L), THH12, close up showing growth laminar along the posterobasal margin (IY134-037). (*C*), Sc element, AM F.135816 (same specimen as Fig. 12G, H), THH9, closing up showing fine growth laminar on the posterior face (IY134-049). *D*,*E*, Sa element, AM F.135048, THH7, (*D*), close up showing fine growth laminar on the posterior face (IY119-006), (*E*), close up showing the small ring-like node representing the initial stage of the element (IY119-012). Scale bars 10 μm.

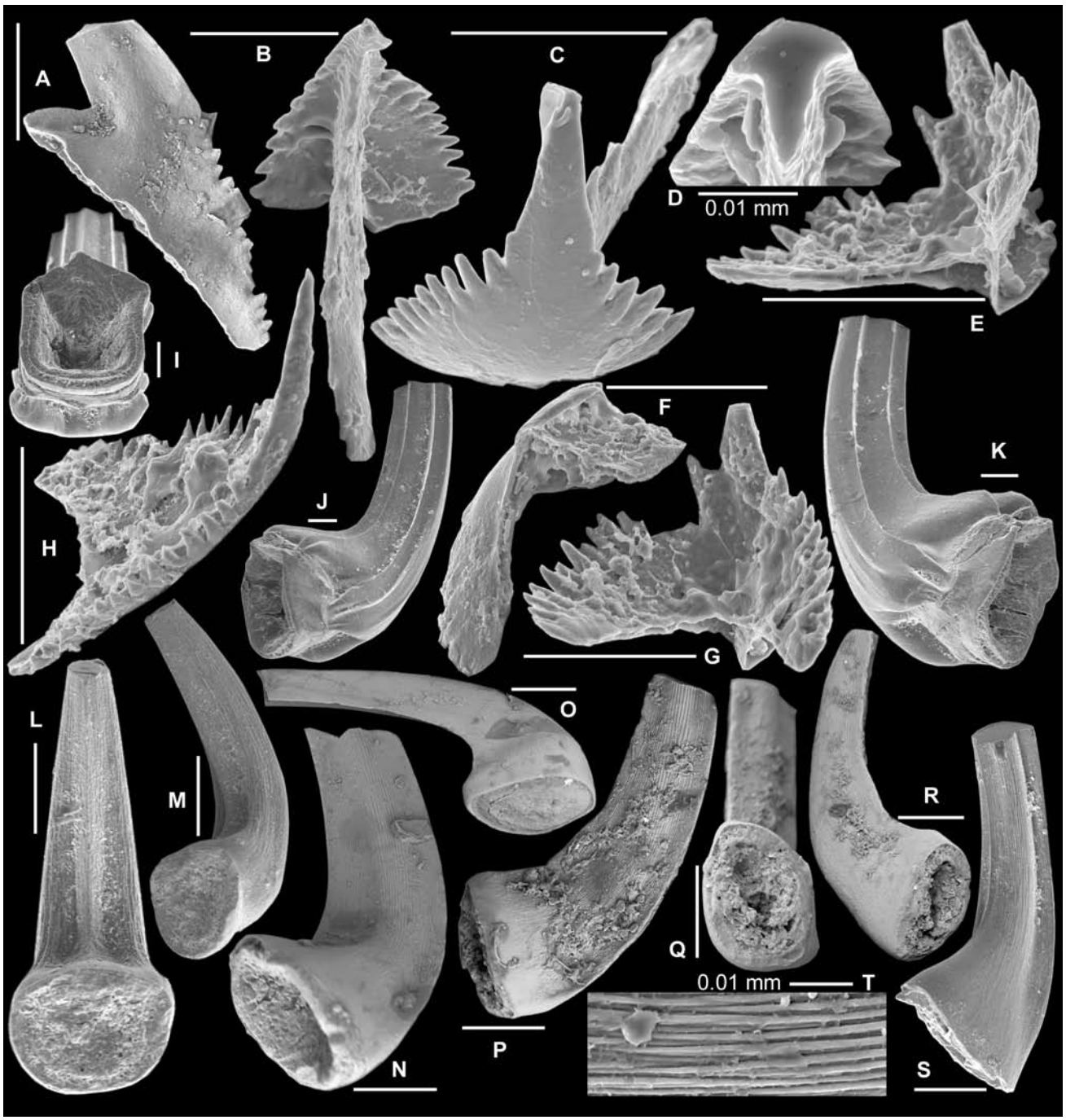

Fig. 15. *A–H*, *Stiptognathus borealis* (Repetski, 1982). (*A*), M element, CPC39902, WCB705/243, posterior view (IY129-033). *B–D*, Sa element; B,C, CPC39903, WCB705/243, (*B*), upper-posterior view (IY118-006), (*C*), upper-anterior view (IY118-007); (*D*), CPC39904, WCB705/243, upper view showing the cross section of the cusp (IY118-004). *E–G*, Sb element, E,G, CPC39905, WCB705/133, (*E*), basal-posterior view (IY117-041), (*G*), posterior view (IY117-039). (*F*), CPC39906, WCB705/243, basal view (IY118-015). (*H*), Pb element, CPC39907, WCB705/243, antero-inner lateral view (IY118-008). *I–K*, *Triangulodus bifidus* Zhen in Zhen *et al*., 2006. Sd element, CPC39908, WCB705/133, (*I*), basal view (IY116-056), (*J,K*), posterolateral views (IY116-058, IY116-057). *L–T*, *Semiacontiodus* sp. cf. *S. cornuformis* (Sergeeva, 1963). *L,M*, Sa element, CPC39909, WCB705/133, (*L*), posterior view (IY126-027); (*M*), posterolateral view (IY126-028). *N,O*, Sb element; (*N*), CPC39910, 161–166 m, inner lateral view (IY132-012); (*O*), CPC39911, 161–166 m, outer lateral view (IY132-014). *P–T*, Sc element; *P–R*, CPC39912, 161–166 m, (*P*), inner lateral view (IY132-016); (*Q*), basal view (IY132-018); (*R*), outer lateral view (IY132-017). *S,T*, CPC39913, WCB705/133, (*S*), inner lateral view (IY127-018); (*T*), close up showing fine striae (IY127-019). Scale bars 100 µm unless otherwise indicated.

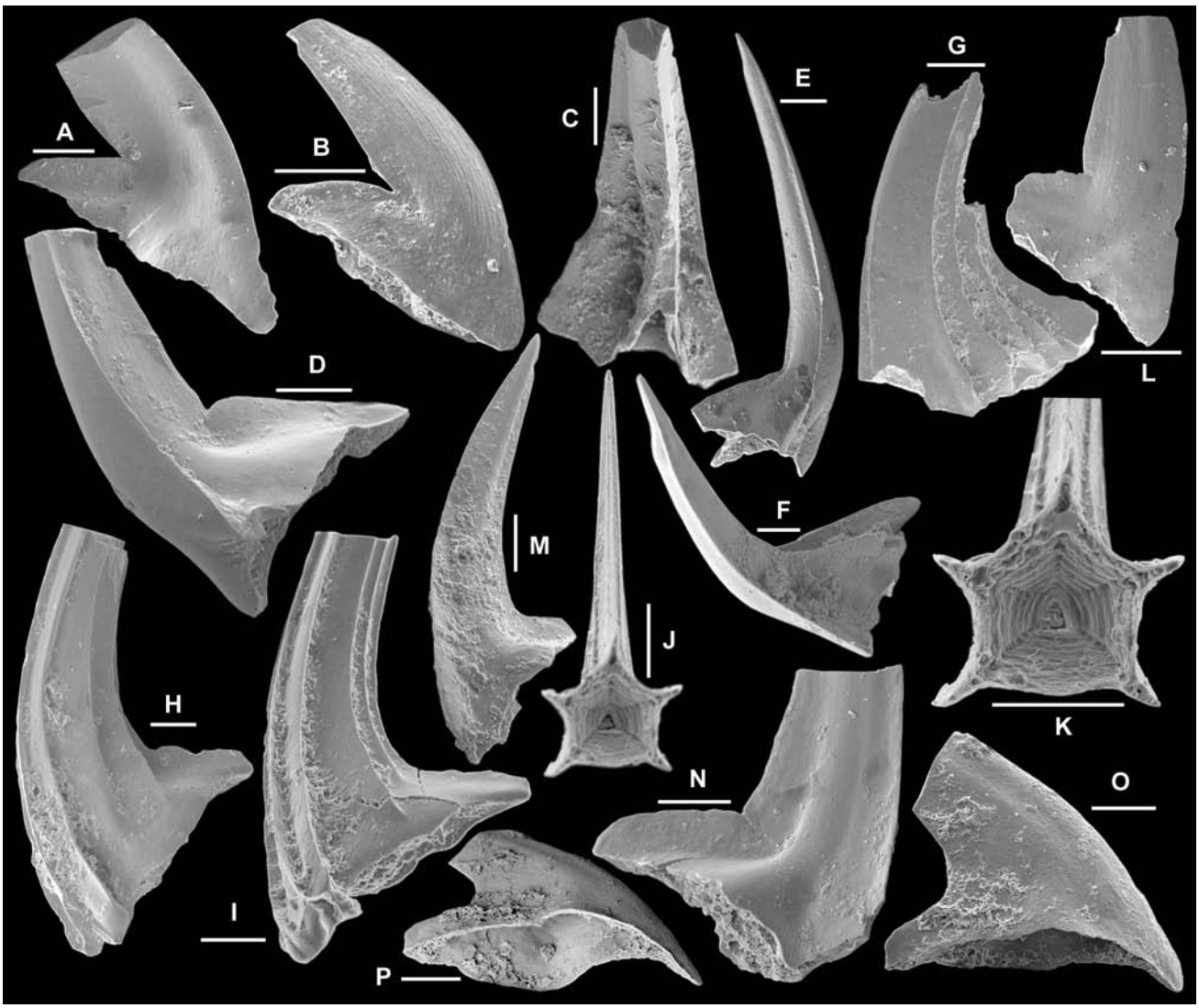

Fig. 16. *Tropodus australis* (Serpagli, 1974). *A,B*, M element; (*A*), CPC39914, WCB705/243, posterior view (IY128-032); (*B*), CPC39915, WCB705/243, anterior view (IY129-007). (*C*), Sa element, CPC39916, WCB705/243, posterior view (IY128-034). (*D*), Sb1 element (tricostate), CPC39917, WCB705/243, outer lateral view (IY128-033). *E,F*, Sb2 element (four costate); (*E*), CPC39918, WCB705/243, outer lateral view (IY128-038); (*F*), CPC39919, WCB705/243, inner lateral view (IY128-036). *G–I*, Sc element; (*G*), CPC39920, WCB705/243, outer lateral view (IY129-003); (*H*), CPC39921, WCB705/243, inner lateral view (IY129-022); (*I*), CPC39922, WCB705/243, inner lateral view (IY118-032). *J,K*, Sd element, CPC39923, WCB705/243, (*J*), basal view (IY118-033), (*K*), basal view close up showing the lamellar structure in the basal cavity (IY118-034). *L–N*, Pa element; (*L*), CPC39924, WCB705/243, outer lateral view (IY128-028); (*M*), CPC39925, WCB705/243, inner lateral view (IY128-022); (*N*), CPC39926, WCB705/243, inner lateral view (IY128-029). *O,P*, Pb element, CPC39927, WCB705/243; (*O*), outer lateral view (IY129-031), (*P*), basal view (IY129-030). Scale bars 100 μm.

Serratognathus diversus An, 1981

Figs 12–14

Serratognathus sp. A An *et al*., 1981: pl. 1, fig. 10.
Serratognathus diversus An, 1981: 216, pl. 2, figs 23, 27, 30; Zhen *et al*., in press a: figs 10A–K, 11A–K, 12D–M (*cum syn.*).
Serratognathus obliquidens Chen, Chen & Zhang, 1983: 136, pl. 1, fig. 18.
Serratognathus tangshanensis Chen, Chen & Zhang, 1983: 136–137, pl. 1, figs 14–17; Chen & Zhang, 1989: 223, pl.5, fig. 12.

Remarks. Both *Serratognathus obliquidens* and *S. tangshanensis* were erected as form species from the Honghuayuan Formation exposed in the Nanjing Hills (Chen *et al*., 1983). We consider them to be junior synonyms of *S. diversus*, representing the asymmetrical elements (Sb + Sc) of our current notation.

Based on a large collection of *S. diversus* from the Honghuayuan Formation, Zhen *et al*. (in press a) recognized a trimembrate apparatus including symmetrical Sa, asymmetrical Sb and strongly asymmetrical Sc elements (Fig. 12). Material of *S. bilobatus* from the Emanuel Formation shows the same apparatus. Morphologically, *S. diversus* and *S. bilobatus* are closely comparable except that the former has a much more prominent, laterally compressed cusp. Their elements are resembling a half-cut onion with a posteriorly located cusp enveloped anterolaterally by numerous overlapping laminar layers (varying from 6 to 20, see Fig. 13). The upper margins of these laminae are progressively lower anterolaterally. Laminae are ornamented with

tooth-like denticles (Fig. 13) along their anterior and lateral margins, and by blunt node-like denticles along the posterior margins (Fig. 14D). Underneath each specimen is a wide, smooth, distally arched basal face (Fig. 12A, G), which is crescentic in outline and divided anteroposteriorly into two lobes (lateral processes; Fig. 13 A–E, K) by a broad, median groove. Typically a small ring-like node underneath the cusp represents the initial stage of the element (Figs 13N, 14E), without basal cavity.

Natural breakage surfaces on some of the specimens show these laminar layers to be tightly compacted (Fig. 12G, H) with partitions generally observed only near the edge of each layer (Fig. 12E–H). In most cases, no microstructure is observable on the surface of the breakage. However, some specimens show fine laminations (growth lamellae) formed by flattened crystallites (Fig. 12I).

Serratognathus extensus Yang in An *et al*., 1983 differs from *S. diversus* in having a more robust cusp and a long, laterally extended process on each side. This species is similar to *S. diversus* and *S. bilobatus* in that the anterior face bears 2–3 rows of denticles that extend continuously from the end of one lateral process to the other, and in lack of a basal cavity. Yang's type material included 14 specimens from the Liangjiashan Formation in Hebei Province (An *et al*., 1983, tables 6–7). An *et al*. (1983, p. 26) suggested that *S. extensus* might be directly evolved from *S. bilobatus*, and recognized the *S. extensus* Zone succeeding the *S. bilobatus* Zone in the Liangjiashan Formation.

Tropodus Kennedy, 1980

Chionoconus Smith, 1991: 22.

Type species. *Tropodus comptus* (Branson & Mehl, 1933).

Remarks. *Tropodus* Kennedy, 1980 is treated herein as a valid genus, having a rather different species apparatus as that of *Acodus*, particularly its S elements that exhibit a much wider variation characterized by the occurrence of multi-costate elements, and the P elements typically with weaker development of a lateral costa that may be represented by a broad carina. *Tropodus* was proposed to consist of a bimembrate apparatus (comprising comptiform and pseudoquadratiform elements) with *Paltodus comptus* Branson & Mehl, 1933 as the type species (Kennedy, 1980). Although the genus was originally defined as consisting of a symmetry transition series of elements bearing "three or more, prominent keel-like costae" (Kennedy, 1980, p. 65), both elements of his revised *T. comptus* have five costae, likely representing only part of a species apparatus. The comptiform element (= Sc herein) was represented by the form species *P. comptus*, an asymmetrical element with costate anterior and posterior margins, and with two costae on the outer face and one on the inner face (Kennedy, 1980, pl. 2, figs 21–24), and the pseudoquadratiform element (= Sd herein) by the form species *Scolopodus pseudoquadratus* Branson & Mehl, 1933, a symmetrical quinquicostate element with a broad anterior face and a costate posterior margin (Kennedy, 1980, pl. 2, figs 25–27).

The other species originally included in *Tropodus* was *Walliserodus australis* which was defined as consisting of a transitional series from tricostate to multicostate elements (Serpagli, 1974, p. 89). Kennedy (1980) admitted that "the two types of elements in *T. comptus* are very similar to two of the many morphologies of elements in *T. australis* (Serpagli, 1974)" although the latter presented "a multitude of variably costate forms." Serpagli (1974) originally defined a quinquimembrate apparatus for *T. australis* including asymmetrical tricostate (= Sb1 herein), asymmetrical quadricostate (= Sb2 herein), strongly asymmetrical, laterally compressed multicostate (= Sc herein) and a nearly symmetrical quinquicostate (= Sd) elements; Sa, P and M elements were originally not recognized in either species.

Based on material from the Cow Head Group of Newfoundland, Bagnoli *et al*. (1988) and Stouge & Bagnoli (1988) included P and M elements in the species apparatus of *Tropodus*. Stouge & Bagnoli (1988) also revised both *T. comptus* and *T. sweeti* (Serpagli, 1974), and suggested that *W. australis* proposed by Serpagli (1974) comprised elements belonging to both *T. comptus* and *T. sweeti*. As Smith (1991) correctly pointed out, distinguishing between S elements belonging to these species is rather uncertain, as Stouge & Bagnoli (1988) had included the holotype (tricostate element) of *W. australis* in the synonymy lists of both *T. comptus* and *T. sweeti*. However, the P elements they defined for *T. comptus* and *T. sweeti* show remarkable differences. The P elements of *T. comptus* illustrated from the Cow Head Group (Stouge & Bagnoli, 1988, pl. 16, fig. 2) and also from Utah (Ethington & Clark, 1982, text-fig. 22, pl. 11, figs 6, 7) are more or less scandodiform bearing a smooth, convex outer face and a concave inner face with a broad, prominent mid carina, while the P element of *T. sweeti* is a typical acodiform element with a prominent costa on one side (Serpagli, 1974, pl. 14, figs 13, 14, pl. 24, figs 8–10). Smith (1991) restricted *Tropodus* to Kennedy's original definition by including only costate elements in the species apparatus and proposed *Chionoconus* to accommodate those elements which Stouge & Bagnoli (1988) defined as the P elements of *T. comptus*.

Zhen *et al*. (2004) reported the occurrence of *T. Australis* (assigned to *T. comptus*) and *T. sweeti* from two samples within the Early Ordovician Hensleigh Siltstone in central New South Wales. The P and M elements of both these species are comparable with those described by Serpagli (1974) from the San Juan Formation of Precordilleran Argentina and by Stouge & Bagnoli (1988) from Newfoundland. However, Zhen *et al*. (2004), following Ji & Barnes (1994), applied a rather different concept for the S elements by including a symmetrical Sa element in the apparatuses. These studies also raised uncertainties about the definition of the constituent species of *Tropodus*. Firstly, if P elements of *Tropodus* are confined to "scandodiform" elements as Stouge & Bagnoli (1988) originally proposed, *T. sweeti* should be excluded from it. Secondly, although Kennedy (1980) suggested that *Triangulodus* consisted of hyaline elements, if *Tropodus* is considered as bearing "scandodiform" P elements, it would be very similar to *Triangulodus*, if it is not considered as a junior synonym of the latter. Among the specimens from the Hensleigh Siltstone, two types of P elements were recognized for *T. australis* (Zhen *et al*., 2004). Both Pa and Pb elements

have a broad convex outer face and a concave inner face with a thin anterior margin curved inward. The lateral costa is weak, and may even be represented only as a broad carina on the inner side of the Pa element (Zhen *et al*., 2004, pl. 1, figs 1, 3) which is comparable with those illustrated by Stouge & Bagnoli (1988, pl. 16, fig. 2)and those from the Emanuel Formation (Fig. 16L–P). However, the lateral costa is plainly evident in the Pb element (Zhen *et al*., 2004, pl. 1, fig. 4). Similar variations among the P elements of *T. comptus* were also observed in the material from the St. George Group (Ji & Barnes, 1994). Therefore, *Tropodus* is defined herein as consisting of a geniculate M element, a series of highly variable S elements (in respect to the number of the costae), and acodiform P elements with a lateral costa on the inner side varying from weak to well developed.

Tropodus australis (Serpagli, 1974)

Fig. 16A–P

Walliserodus australis Serpagli, 1974: 89–91, pl. 19, figs 5a–10c, pl. 29, figs 8–15, text-figs 23, 24.

Tropodus australis (Serpagli).—Albanesi *et al*., 1998: 151, pl. 13, figs 12–18.

Tropodus comptus australis (Serpagli).—Stouge & Bagnoli, 1988: 141, 142, pl. 16, figs 3–5; Löfgren, 1993: fig. 9: o, s, t; Lehnert, 1993: pl. 4, fig. 5; Lehnert, 1995: 129, 130.

Acodus comptus (Branson & Mehl, 1933).—Zhen *et al*., 2004: 50, 51, pl. 1, figs 1–19.

Scolopodus ?rex Lindström.—Percival *et al*., 1999: 13, fig. 8.9.

Tropodus ?sweeti (Serpagli).—Percival *et al*., 1999: 13, fig. 8.10.

Material. 190 specimens from three samples (Table 1).

Remarks. Specimens from the Emanuel Formation are identical with those recovered from the Hensleigh Siltstone of central New South Wales (Zhen *et al*., 2004, pl. 1, figs 1–19). Stouge & Bagnoli (1988) regarded *W. australis* as a subspecies of *T. comptus*. In the Emanuel Formation samples, only one species of *Tropodus*, *T. australis* is represented, exhibiting similar variation of the S elements (Fig. 16C–K) as was documented by Serpagli (1974), and the P elements (Fig. 16L–P) that are comparable with those described by Stouge & Bagnoli (1988) from the Cow Head Group of Newfoundland.

Tropodus australis differs from typical *T. comptus* of the North American Mid-continent (Kennedy, 1980; Ethington & Clark, 1982; Landing & Wesrop, 2006) mainly in having a strongly laterally compressed, muti-costate (Sc) element. Landing & Westrop (2006) documented *T. comptus* from the Fort Cassin (Early Ordovician, Floian) of northeastern New York, and defined it as consisting of a septimembrate apparatus including S, M and P elements, and also illustrated a scandodiform element as representing the Sc position (see Landing & Westrop, 2006, fig. 6.15). In the study of conodont faunas from the Jefferson City and other equivalent units in Oklahoma (Kindblade), Ethington (2009, per. com.) recognized the possible P elements of *T. comptus* and noticed their considerable difference from those of *T. australis* illustrated herein from the Emanuel Formation. He suggested that elements of *T. australis* tended to be heavier whereas those of *T. comptus* were more subdued.

ACKNOWLEDGMENTS. Study by YYZ was partially supported by the CAS/SAFEA International Partnership Program for Creative Research Teams. Scanning electron microscope photographs were prepared in the Electron Microscope Unit of the Australian Museum. Dr Ian Percival is thanked for carefully reading and helping with linguistic expression on an early version of the manuscript. G.S Nowlan, R.L. Ethington and S.A. Leslie are thanked for their careful and constructive reviews of the manuscript. This is a contribution to IGCP Project 503: Ordovician Palaeogeography and Palaeoclimate.

References

Albanesi, G.L., M.A. Hünicken & C.R. Barnes, 1998. Bioestratigrafía, biofacies y taxonomia de conodontes de las secuencias ordovícicas del Cerro Porterillo, Precordillera central de San Juan, R. Argentina. *Actas de la Academia Nacional de Ciencias* 12: 1–249.

An, T.X., 1981. Recent progress in Cambrian and Ordovician conodont biostratigraphy of China. *Geological Society of America Special Paper* 187: 209–226.

An, T.X., 1987. *Early Palaeozoic conodonts from South China*. Peking University Publishing House, Beijing, 238 pp. (in Chinese with English abstract).

An, T.X., & L.S. Ding, 1982. Preliminary studies and correlations on Ordovician conodonts from the Ningzhen Mountains, China. *Acta Petroleum Sinica* 3(4): 1–11 (in Chinese).

An, T.X., & L.S. Ding, 1985. Ordovician conodont biostratigraphy in Hexian, Anhui Province. *Geological Review* 31: 1–12.

An, T.X., G.Q. Du & Q.Q. Gao, 1985. *Ordovician conodonts from Hubei*. Geological Publishing House, Beijing, 64 pp. (in Chinese with English abstract).

An, T.X., G.Q. Du, Q.Q. Gao, X.B. Chen & W.T. Li, 1981. Ordovician conodont biostratigraphy of the Huanghuachang area of Yichang, Hubei. In *Selected Papers of the First Symposium of the Micropalaeontological Society of China*, Micropalaeontological Society of China, ed., Science Press, Beijing, 105–113 (in Chinese).

An, T.X., F. Zhang, W.D. Xiang, Y.Q. Zhang, W.H. Xu, H.J. Zhang, D.B. Jiang, C.S. Yang, L.D. Lin, Z.T. Cui & X.C. Yang, 1983. *The Conodonts of North China and the Adjacent Regions*. Science Press, Beijing, 223 pp. (in Chinese with English abstract).

An, T.X., & S.C. Zheng, 1990. *The conodonts of the marginal areas around the Ordos Basin, north China*. Science Press, Beijing, 199 pp. (in Chinese with English abstract).

Bagnoli, G., S. Stouge & M. Tongiorgi, 1988. Acritarchs and conodonts from the Cambro-Ordovician Furuhäll (Köpingsklint) Section (Öland, Sweden). *Revista Italiana di Paleontologia e Stratigrafia* 94(2): 163–248.

Balfour, F.M., 1880–1881. *A treatise on Comparative Embryology*. Two Volumes. Macmillan & Co., London.

Bergström, S.M., 1988. On Pander's Ordovician conodonts: distribution and significance of the *Prioniodus elegans* fauna in Baltoscandia. *Senckenbergiana lethaea* 69: 217–251.

Bergström, S.M., A. Löfgren & J. Maletz, 2004. The GSSP of the second (upper) stage of the Lower Ordovician Series: Diabasbrottet at Hunneberg, Province of Västergötland, southwestern Sweden. *Episodes* 27(4): 265–272.

Branson, E.R., & M.G. Mehl, 1933. Conodont studies. *University of Missouri Studies* 8: 1–349.

Brock, G.A., & L.E. Holmer, 2004. Early Ordovician lingulate brachiopods from the Emanuel Formation, Canning Basin, Western Australia. *Memoir of the Association of Australasian Palaeontologists* 30: 113–132.

Brown, I.A., 1964. An Ordovician cystoid (Pelmatozoa, Echinodermata) from Western Australia. *Proceedings of the Royal Society of Western Australia* 47: 3–7.

Chen, M.J., Y.T. Chen & J.H. Zhang, 1983. Ordovician conodont sequence in Nanjing Hills. *Journal of Nanjing University, Natural Sciences* 1983 (1): 129–139 (in Chinese with English abstract).

Chen, M.J., & J.H. Zhang, 1989. Ordovician conodonts from the Shitai region, Anhui. *Acta Micropalaeontologica Sinica* 6(3): 213–228 (in Chinese with English abstract).

Chen, X., J.Y. Rong, X.F. Wang, Z.H. Wang, Y.D. Zhang & R.B. Zhan, 1995. Correlation of the Ordovician rocks of China: charts and explanatory notes. *International Union of Geological Sciences, Publication* 31: 1–104.

Chen, X., & Z.H. Wang, 1993. The base of Arenig Series in China. *Newsletters on Stratigraphy* 29: 159–164.

Choi, D.K., S.K. Chough, Y.K. Kwon & S.B. Lee, 2005. Excursion 8: Taebaeksan Basin, Korea: Cambrian-Ordovician Joseon Supergroup of the Taebaeksan Basin, Korea. 265–300. *In Cambrian System of China and Korea—Guide to Field Excursions*, ed. Peng, S.C., L.E. Babcock & M.Y. Zhu. China University of Science and Technology Press, Hefei.

Choi, D.K., D.H. Kim & J.W. Sohn, 2001. Ordovician trilobite faunas and depositional history of the Taebaeksan Basin, Korea: implications for palaeogeography. *Alcheringa* 25: 53–68.
http://dx.doi.org/10.1080/03115510108619213

Clark, D.L., W.C. Sweet, S.M. Bergström, G. Klapper, R.L. Austin, F.H.T. Rhodes, K.J. Müller, W. Ziegler, M. Lindström, J.F. Miller & A.G. Harris, 1981. Conodonta. In *Treatise on Invertebrate Paleontology, part W, Miscellanea, supplement 2*, ed. R.A. Robison. Geological Society of America, Boulder and University of Kansas, Lawrence, 202 pp.

Ding, L.S., 1987. Preliminary probes into Ordovician conodont biostratigraphy from the Kunshan area, Jiangsu, China. In *Symposium on petroleum stratigraphy and palaeontology* (1987), 41–53, Geological Publishing House, Beijing.

Ethington, R.L., & D.L. Clark, 1982. Lower and Middle Ordovician conodonts from the Ibex area, western Millard County, Utah. *Brigham Young University, Geological Studies* 28(2): 1–160.

Ethington, R.L., O. Lehnert & J.E. Repetski, 2000. *Stiptognathus* new genus (Conodonta: Ibexian, Lower Ordovician), and the apparatus of *Stiptognathus borealis* (Repetski, 1982). *Journal of Paleontology* 74: 92–100.
http://dx.doi.org/10.1666/0022-3360(2000)074<0092:SNGCIL>2.0.CO;2

Fåhraeus, L.E., 1982. Recognition and redescription of Pander's (1856) *Scolopodus* (form) species—constituents of multi-element taxa (Conodontophorida, Ordovician). *Geologica et Palaeontologica* 16: 19–28.

Gilbert-Tomlinson, J., 1973. The Lower Ordovician gastropod *Teiichispira* in Northern Australia. *Bureau of Mineral Resources, Geology & Geophysics, Bulletin* 126: 65–88.

Graves, R.W., & S. Ellison, 1941. Ordovician conodonts of the Marathon Basin, Texas. *University of Missouri, School of Mines and Metallurgy, Bulletin* (Ser.) 14: 1–26.

Guppy, D.G., A.W. Lindner, J.H. Rattigan & J.N. Casey, 1958. The geology of the Fitzroy Basin, Western Australia. *Bureau of Mineral Resources, Geology and Geophysics, Bulletin* 36: 1–116.

Guppy, D.G., & A.A. Öpik, 1950. Discovery of Ordovician rocks, Kimberley Division, W.A. *Australian Journal of Science* 12: 205–206.

Henderson, S.D., 1963. Bore BMR 3 Prices Creek. In Henderson, S.D., M.A. Condon & L.V. Bastian, Stratigraphic drilling, Canning Basin, Western Australia. *Bureau of Mineral Resources, Geology and Geophysics, Report* 60: 46–51.

Hocking, R.M., I.A. Copp, P.E. Playford & R.H. Kempton, 1996. The Cadjebut Formation: a Givetian evaporitic precursor to Devonian reef complexes of the Lennard Shelf, Canning Basin, Western Australia. *Geological Survey of Western Australia, Annual Review* 1995–1996: 48–55.

Huang, B.C., R.X. Zhu, Y. Otofuji & Z.Y. Yang, 2000. The Early Paleozoic paleogeography of the North China block and the other major blocks of China. *Chinese Science Bulletin* 45(12): 1057–1065.
http://dx.doi.org/10.1007/BF02887174

Jell, P.A., C.F. Burrett, B. Sait & E.L. Yochelson, 1984. The Ordovician bellerophontid *Peelerophon oehlerti* (Bergeron) from Argentina, Australia and Thailand. *Alcheringa* 8: 169–176.
http://dx.doi.org/10.1080/03115518408618941

Ji, Z.L., & C.R. Barnes, 1994. Lower Ordovician conodonts of the St. George Group, Port au Port Peninsula, western Newfoundland, Canada. *Palaeontographica Canadiana* 11: 1–149.

Johnston, D.I., & C.R. Barnes, 2000. Early and Middle Ordovician (Arenig) conodonts from St. Pauls Inlet and Martin Point, Cow Head Group, western Newfoundland, Canada. 2. Systematic paleontology. *Geologica et Palaeontologica* 34: 11–87.

Kennedy, D.J., 1980. A restudy of conodonts described by Branson and Mehl, 1933, from the Jefferson City Formation, Lower Ordovician, Missouri. *Geologica et Palaeontologica* 14: 45–76.

Landing, E., & S.R. Westrop, 2006. Lower Ordovician faunas, stratigraphy, and sea-level history of the middle Beekmantown Group, northeastern New York. *Journal of Paleontology* 80(5): 958–980.
http://dx.doi.org/10.1666/0022-3360(2006)80[958:LOFSAS]2.0.CO;2

Laurie, J.R., & J.H. Shergold, 1996a. Early Ordovician trilobite. taxonomy and biostratigraphy of the Emanuel Formation, Canning Basin, Western Australia. Part 1. *Palaeontographica Abteilung A* 240: 65–103.

Laurie, J.R., & J.H. Shergold, 1996b. Early Ordovician trilobite. taxonomy and biostratigraphy of the Emanuel Formation, Canning Basin, Western Australia. Part 2. *Palaeontographica Abteilung A* 240: 105–144.

Lee, H.Y., 1970. Conodonten aus der Choson-Gruppe (Unteres Ordovizium) von Korea. *Neues Jahrbuch für Geologie und Paläontologie, Abhandlungen* 136(3): 303–344.

Lee, H.Y., 1975. Conodonts from the Dumugol Formation (Lower Ordovician), South Korea. *Journal of the Geological Society of Korea* 11(2): 75–98.

Legg, D.P., 1976. Ordovician trilobites and graptolites from the Canning Basin, Western Australia. *Geologica et Palaeontologica* 10: 1–58.

Lehnert, O., 1993. Bioestratigrafía de los conodontes arenigianos de la Formación San Juan en la localidad de Niquivil (Precordillera Sanjuanian, Argentina) y su correlación intercontinental. *Revista Española de Paleontología* 8(2): 153–164.

Lehnert, O., 1995. Ordovizische Conodonten aus der Präkordillere Westargentiniens: Ihre Bedeutung für Stratigraphie und Paläogeographie. *Erlanger Geologische Abhandlungen* 125: 1–193.

Lindström, M., 1955. Conodonts from the lowermost Ordovician strata of south-central Sweden. *Geologiska Föreningens i Stockholm Förhandlingar* 76: 517–604.

Lindström, M., 1971. Lower Ordovician conodonts of Europe. In *Symposium on Conodont Biostratigraphy*, ed. W.C. Sweet & S.M. Bergström. *Geological Society of America, Memoir* 127: 21–61.

Löfgren, A., 1978. Arenigian and Llanvirnian conodonts from Jämtland, northern Sweden. *Fossils and Strata* 13: 1–129.

Löfgren, A., 1993. Conodonts from the Lower Ordovician at Hunneberg, south-central Sweden. *Geological Magazine* 130: 215–232.

Löfgren, A., 1997. Reinterpretation of the Lower Ordovician conodont apparatus *Paroistodus*. *Palaeontology* 40(4): 913–929.

Löfgren, A., 1999. The Ordovician conodont *Semiacontiodus cornuformis* (Sergeeva, 1963) and related species in Baltoscandia. *Geologica et Palaeontologica* 33: 71–91.

Löfgren, A., & T.J. Tolmacheva, 2003. Taxonomy and distribution of the Ordovician conodont *Drepanodus arcuatus* Pander, 1856, and related species. *Paläontologische Zeitschrift* 77(1): 203–221.

McTavish, R.A., 1973. Prioniodontacean conodonts from the Emanuel Formation (Lower Ordovician) of Western Australia. *Geologica et Palaeontologica* 7: 27–58.

McTavish, R.A., & D.P. Legg, 1976. The Ordovician of the Canning Basin, Western Australia. In *The Ordovician System: proceedings of a Palaeontological Association Symposium, Birmingham, September 1974*, ed. M.G. Bassett, pp. 447–478. The Palaeontological Association, University of Wales Press.

Metcalfe, I., 1980. Ordovician conodonts from the Kaki Bukit area, Perlis, West Malaysia. *Warta Geologi* 6: 63–68.

Metcalfe, I., 2004. Colour and textural alteration of Palaeozoic and Triassic conodonts from Peninsular Malaysia: implications for tectonic evolution and hydrocarbon generation. *Courier Forschungsinstitut Senckenberg* 245: 261–279.

Miller, J.F., 1969. Conodont fauna of the Notch Peak Limestone (Cambro-Ordovician), House Range, Utah. *Journal of Paleontology* 43: 413–439.

Nicoll, R.S., 1990. The genus *Cordylodus* and a latest Cambrian-earliest Ordovician conodont biostratigraphy. *BMR Journal of Australian Geology & Geophysics* 11: 529–558.

Nicoll, R.S., 1992. Analysis of conodont apparatus organisation and the genus *Jumudontus* (Conodonta), a coniform-pectiniform apparatus structure from the Early Ordovician. *BMR Journal of Australian Geology & Geophysics* 13: 213–228.

Nicoll, R.S., & R.L. Ethington, 2004. *Lissoepikodus nudus* gen. et sp. nov. and *Oepikodus cleftus* sp. nov., new septimembrate conodont taxa from the Early Ordovician of Australia and Nevada. *Courier Forschungsinstitut Senckenberg* 245: 427–461.

Nicoll, R.S., J.R. Laurie & M.T. Roche, 1993. Revised stratigraphy of the Ordovician (late Tremadoc-Arenig) Prices Creek Group and Devonian Poulton Formation, Lennard Shelf, Canning Basin, Western Australia. *AGSO Journal of Australian Geology & Geophysics* 14: 65–76.

Nicoll, R.S., & I. Metcalfe, 2001. Cambrian to Permian conodont biogeography in East Asia-Australasia. In *Faunal and floral migrations and evolution in SE Asia-Australasia*, ed. I. Metcalfe, J.M.B. Smith, M. Morwood & I. Davidson, pp. 59–72. Balkema, Lisse.

Norford, B.S, D.E. Jackson & G.S. Nowlan, 2002. Ordovician stratigraphy and faunas of the Glenogle Formation, southeastern British Columbia. Geological Survey of Canada Bulletin 569: 1–84.

Nowlan, G.S., A.D. McCracken & M.J. McLeod, 1997. Tectonic and paleogeographic significance of Late Ordovician conodonts in the Canadian Appalachians. *Canadian Journal of Earth Sciences* 34: 1521–1537.

Pander, C.H., 1856. *Monographie der fossilen Fische des Silurischen Systems der Russisch-Baltischen Gouvernements*. Akademie der Wissenschaften, St. Petersburg, 91 pp.

Percival, I.G., E.J. Morgan & M.M. Scott, 1999. Ordovician stratigraphy of the northern Molong Volcanic Belt: new facts and figures. *Geological Survey of New South Wales, Quarterly Notes* 108: 8–27.

Percival, I.G., Y.Y. Zhen & B.D. Webby, 2003. Early Ordovician conodont distribution from craton to basin and island terranes in east Gondwana. Proceedings of the 9th International Symposium on the Ordovician System, San Juan, Argentina, 2003. In *Ordovician from the Andes*, ed. G.L. Albanesi, M.S. Beresi & S.H. Peralta. *INSUGEO, Serie Correlación Geológica* 17: 533–537.

Purcell, P.G., ed., 1984. The Canning Basin, W.A. *Proceedings of Geological Society of Australia/Petroleum Exploration Society of Australia Synmposium*. Perth, 253–275.

Pyle, L.J., & C.R. Barnes, 2002. Taxonomy, Evolution, and Biostratigraphy of Conodonts from the Kechika Formation, Skoki Formation, and Road River Group (Upper Cambrian to Lower Silurian), Northeastern British Columbia. 227 p., NRC Research Press, Ottawa, Ontario, Canada.

Repetski, J.E., 1982. Conodonts from E1 Paso Group (Lower Ordovician) of westernmost Texas and southern New Mexico. *New Mexico Bureau of Mines & Mineral Resources, Memoir* 40: 1–121.

Schallreuter, R.E.L., 1993a. On *Eopilla nulea* Schallreuter n.sp. *Stereo Atlas of Ostracod Shells* 20, part 2 (28), 117–120.

Schallreuter, R.E.L., 1993b. On *Eopilla ingelorae* Schallreuter n.sp. *Stereo Atlas of Ostracod Shells* 20, part 2 (29), 121–124.

Seo, K.S., H.Y. Lee & R.L. Ethington, 1994. Early Ordovician conodonts from the Dumugol Formation in the Baegunsan Syncline, eastern Yeongweol and Samcheog areas, Kangweon-Do, Korea. *Journal of Paleontology* 68(3): 599–616.

Sergeeva, S.P., 1963. Conodonts from the Lower Ordovician of the Leningrad region. *Paleontologicheskiy Zhurnal, Akademiya Nauk SSSR* 2: 93–108.

Serpagli, E., 1974. Lower Ordovician conodonts from Precordilleran Argentina (Province of San Juan). *Bollettino della Società Paleontologica Italiana* 13: 17–98.

Smith, M.P., 1991. Early Ordovician conodonts of East and North Greenland. *Meddelelser om Grønland, Geoscience* 26: 1–81.

Stouge, S., & G. Bagnoli, 1988. Early Ordovician conodonts from Cow Head Peninsula, western Newfoundland. *Palaeontographica Italica* 75: 89–179.

Stouge, S., & G. Bagnoli, 1999. The suprageneric classification of some Ordovician prioniodontid conodonts. In *Studies on Conodonts—Proceedings of the Seventh European Conodont Symposium, Bologna-Modena, 1998*, ed. E. Serpagli. *Bollettino della Società Paleontologica Italiana* 37: 145–158.

Sweet, W.C., 1988. *The Conodonta: Morphology, Taxonomy, Paleoecology, and Evolutionary History of a Long-Extinct Animal Phylum*. Oxford: Clarendon Press.

Sweet, W.C., & S.M. Bergström, 1972. Multielement taxonomy and Ordovician conodonts. *Geologica et Palaeontologica* SB1: 29–42.

Teichert, C., & B.F. Glenister, 1954. Early Ordovician cephalopod fauna from northwestern Australia. *Bulletin of American Paleontology* 35(150): 1–113.

Thomas, D.E., 1960. The zonal distribution of Australian graptolites. *Journal and Proceedings of the Royal Society of New South Wales* 94: 1–58.

Tolmacheva, T.J., 2006. Apparatus of the conodont *Scolopodus striatus* Pander, 1856 and a re-evaluation of Pander's species of *Scolopodus*. *Acta Palaeontologica Polonica* 51(2): 247–260.

Tolmacheva, T.Y., & A. Löfgren, 2000. Morphology and paleogeography of the Ordovician conodont *Paracordylodus gracilis* Lindström, 1955: comparison of two populations. *Journal of Paleontology* 74(6): 1114–1121.
http://dx.doi.org/10.1666/0022-3360(2000)074<1114:MAPOTO>2.0.CO;2

Tolmacheva, T.Y., & M.A. Purnell, 2002. Apparatus composition, growth, and survivorship of the Lower Ordovician conodont *Paracordylodus gracilis* Lindström, 1955. *Palaeontology* 45(2): 209–228.
http://dx.doi.org/10.1111/1475-4983.00234

Tolmacheva, T.Y., T.N. Koren, L.E. Holmer, L.E. Popov & E. Raevskaya, 2001. The Hunneberg Stage (Ordovician) in the area east of St. Petersburg, north-western Russia. *Paläontologische Zeitschrift* 74(4): 543–561.

Towner, R.R., & D.L. Gibson, 1983. Geology of the onshore Canning Basin, Western Australia. *Bureau of Mineral Resources, Geology and Geophysics, Bulletin* 215: 1–51.

Veevers, J.J., & A.T. Wells, 1961. The geology of the Canning Basin, Western Australia. *Bureau of Mineral Resources, Geology & Geophysics Bulletin* 60: 1–323.

Viira, V., K. Mens & J. Nemliher, 2006. Lower Ordovician Leetse Formation in the North Estonian Klint area. *Proceedings of the Estonian Academy of Sciences, Geology* 55(2): 156–174.

van Wamel, W.A., 1974. Conodont biostratigraphy of the Upper Cambrian and Lower Ordovician of north-western Öland, south-eastern Sweden. *Utrecht Micropalaeontological Bulletins* 10: 1–125.

Wang, C.Y., ed., 1993. *Conodonts of the Lower Yangtze Valley—an index to biostratigraphy and organic metamorphic maturity*. Science Press, Beijing, 326pp. (in Chinese with English summary).

Wang, X.F., X. Chen, X.H. Chen & C.H. Zhu, eds, 1996. *Lexicon of Stratigraphy of China: Ordovician*. Geological Publishing House, Beijing, 126 pp. (Chinese with English abstract).

Wang, Z.H., S.M. Bergström & H.R. Lane, 1996. Conodont provinces and biostratigraphy in Ordovician of China. *Acta Palaeontologica Sinica* 35: 26–59.

Webby, B.D., I.G. Percival, G. Edgecombe, F. Vandenberg, R.Cooper, J. Pickett, J. Pojeta Jr., G. Playford, T. Winchester-Seeto, Y.Y. Zhen, R.S. Nicoll, J.R.P. Ross, R. Schallreuter & G. Young, 2000. Ordovician biogeography of Australasia. In *Palaeobiogeography of Australasian Faunas and Floras*, ed. J. Wright, J. Talent & G. Young. *Association of Australian Palaeontologists, Memoir* 23: 63–126.

Williams, S.H., & R.K. Stevens, 1988. Early Ordovician (Arenig) graptolites of the Cow Head Group, western Newfoundland, Canada. *Palaeontographica Canadiana* 5: 1–167.

Williams, S.H., G.S. Nowlan, C.R. Barnes & S.R. Batten, 1999. The Ledge Section at Cow Head, western Newfoundland: new data and discussion of the graptolite, conodont and chitinozoan assemblages. In *Quo Vadis Ordovician? Short papers of the 8th International Symposium on the Ordovician System*, ed. P. Kraft & O. Fatka. Prague. *Acta Universitatis Carolinae, Geologica* 43: 65–68.

Yu, W., 1993. Ordovician gastropods from the Canning Basin, Western Australia. *Records of the Western Australian Museum* 16: 437–458.

Zhao, Z.X., G.Z. Zhang & J.N. Xiao, 2000. Paleozoic stratigraphy and conodonts in *Xinjiang*. Petroleum Industry Press, Beijing, 340 pp. (in Chinese with English abstract).

Zhen, Y.Y., 2007. Conodont biostratigraphy of the Honghuayuan Formation (late Early Ordovician) in Guizhou, South China. *Acta Palaeontologica Sinica* 46 (Supplement): 537–542.

Zhen, Y.Y., & I.G. Percival, 2003. Ordovician conodont biogeography—reconsidered. *Lethaia* 36: 357–369.
http://dx.doi.org/10.1080/00241160310006402

Zhen, Y.Y., R.S. Nicoll, I.G. Percival, M.A. Hamedi & I. Stewart, 2001. Ordovician Rhipidognathidae (Conodonta) from Australia and Iran. *Journal of Paleontology* 75(1): 186–207.
http://dx.doi.org/10.1666/0022-3360(2001)075<0186:ORCFAA>2.0.CO;2

Zhen, Y.Y., & I.G. Percival, 2006. Late Cambrian–Early Ordovician conodont faunas from the Koonenberry Belt of western New South Wales, Australia. *Memoir of the Association of Australasian Palaeontologists* 32: 267–285.

Zhen, Y.Y., I.G. Percival & B.D. Webby, 2003. Early Ordovician conodonts from western New South Wales, Australia. *Records of the Australian Museum* 55(2): 169–220.
http://dx.doi.org/10.3853/j.0067-1975.55.2003.1383

Zhen, Y.Y., I.G. Percival & B.D. Webby, 2004. Early Ordovician (Bendigonian) conodonts from central New South Wales, Australia. *Courier Forschungsinstitut Senckenberg* 245: 39–73.

Zhen, Y.Y., J.B. Liu & I.G. Percival, 2005. Revision of two prioniodontid species (Conodonta) from the Early Ordovician Honghuayuan Formation of Guizhou, South China. *Records of the Australian Museum* 57(2): 303–320.
http://dx.doi.org/10.3853/j.0067-1975.57.2005.1448

Zhen, Y.Y., I.G. Percival & J.B. Liu, 2006. Early Ordovician *Triangulodus* (Conodonta) from the Honghuayuan Formation of Guizhou, South China. *Alcheringa* 30: 191–212.
http://dx.doi.org/10.1080/03115510608619313

Zhen, Y.Y., J.B. Liu & I.G. Percival, 2007a. Revision of the conodont *Erraticodon hexianensis* from the upper Meitan Formation (Middle Ordovician) of Guizhou, South China. *Palaeontological Research* 11: 145–162.
http://dx.doi.org/10.2517/1342-8144(2007)11[145:ROTCEH]2.0.CO;2

Zhen, Y.Y., I.G. Percival, R.A. Cooper, J.E. Simes & A.J. Wright, 2009. Darriwilian (Middle Ordovician) conodonts from Thompson Creek, Nelson Province, New Zealand. *Memoir of the Association of Australasian Palaeontologists*: in press (*b*).

Zhen, Y.Y., I.G. Percival, J.B. Liu & Y.D. Zhang, 2009. Conodont fauna and biostratigraphy of the Honghuayuan Formation (Early Ordovician) of Guizhou, South China. *Alcheringa* 33: in press (*a*).

Zhen, Y.Y., I.G. Percival, A. Löfgren & J.B. Liu, 2007b. Drepanoistodontid conodonts from the Early Ordovician Honghuayuan Formation of Guizhou, South China. *Acta Micropalaeontologica Sinica* 24(2): 125–148.

Zhou, Z.Y., & R.A. Fortey, 1986. Ordovician trilobites from north and northeast China. *Palaeontographica Abteilung A* 192: 157–210.

Zhou, Z.Y., & Y.Y. Zhen, 2008. Trilobite-constrained Ordovician biogeography of China with reference to the faunal connections with Australia. *Proceedings of the Linnean Society of New South Wales* 129: 183–195.

Zhou, Z.Y., Y.Y. Zhen & S.C. Peng, 2008. A review of Cambrian biogeography of China. In *Advances in trilobite research. Cuadermos del Museo Geominero*, 9, ed. I. Rábano, R. Gozalo & D. Garcia-Bellido. Instituto Geológico y Minero de España, Madrid, 435–442.

Zhylkaidarov, A., 1998. Conodonts from Ordovician ophiolites of central Kazakhstan. *Acta Palaeontologica Polonica* 43: 53–68.

Ziegler, W., ed., 1977. *Catalogue of Conodonts. III*: 1–574. Stuttgart: E. Schweizerbart'sche.

Manuscript submitted 20 January 2009, revised 3 March 2009, and accepted 6 March 2009.